TOPICAL REVIEW — Magnetism, magnetic materials, and interdisciplinary research

Chemical synthesis of magnetic nanocrystals: Recent progress*

Liu Fei(刘 飞)[a], Zhu Jing-Han(朱静菡)[a], Hou Yang-Long(侯仰龙)[a]†, and Gao Song(高 松)[b]

[a] Department of Materials Science and Engineering, College of Engineering, Peking University, Beijing 100871, China
[b] College of Chemistry and Molecular Engineering, Peking University, Beijing 100871, China

(Received 24 July 2013)

Colloidal chemical synthesis of various types of magnetic nanocrystals is discussed with regard to recent discoveries. We first outline the chemical preparation of single-component magnetic nanocrystals with controlled size, shape, and uniformity based on several solution-phase methods, especially thermal decomposition and/or reduction method. Then we discuss the synthetic strategies of multi-component nanocrystals incorporating at least one magnetic component by manipulating heterogeneous nucleation and growth process. Toward the end, approaches for preparing hollow/porous magnetic nanocrystals are highlighted. We believe that the summarized chemical synthesis will pave the way for the future development of extraordinary magnetic nanocrystals.

Keywords: magnetic nanocrystals, chemical synthesis, single-component, multi-component, hollow/porous

PACS: 75.75.cd, 81.16.Be, 81.20.Ka, 61.46.–w **DOI:** 10.1088/1674-1056/22/10/107503

1. Introduction

For past decades, magnetic nanocrystals (NCs) have attracted a great deal of interest due to their extraordinary potential for data storage,[1] catalysis,[2,3] biomedical imaging,[4–8] drug delivery,[9,10] and environmental remediation.[11,12] The properties of the NCs strongly depend on their dimensions, and as a result, their physical properties vary dramatically from their bulk counterparts, which offer various opportunities for wide applications. In terms of magnetic materials, the size-effect will result in the NC which possesses a single magnetic domain and shows superparamagnetic behavior when the temperature is above the blocking temperature.[7,13,14] Superparamagnetic NCs can be easily saturated in the presence of a field, but the magnetization returns to zero upon removal of the field due to thermal fluctuations. This unique feature has proven to be ideal for a broad range of biomedical applications such as targeted drug delivery, localized heating of cancerous cells (hyperthermia), and magnetic resonance imaging (MRI) because aggregation of such NCs can be effectively avoided.[14–18] On the other hand, properties of nanomaterials can also be tuned by varying their shapes.[19] Therefore, to fully exploit the potential of magnetic NCs with desired properties, synthesis of uniformly sized and shaped magnetic NCs is of significant importance.

Recently, synthesis of heterostructured NCs (HNCs) with discrete domains of different materials is becoming an important research direction in nanotechnology.[20–30] Primarily, HNCs incorporating multiple materials, each characterized by unique optical, electric, magnetic, and/or chemical properties, provide multi-functionality that may result in unprecedented applications.[26–31] Additionally, HNCs possessing artificial interfaces, where electronic communication exists across neighboring material sections, can generate synergistically enhanced and/or tunable chemical–physical responses, or even provide novel functions that are not available in single-component materials or structures.[32–35] In particular, electronic interactions at the interface are present in magnetic HNCs, which may lead to variation of the magnetic properties by magnetic exchange-coupling mechanisms and/or induced extra anisotropy.[33,34] Therefore, establishing HNCs with effective bonding junctions among dissimilar nanoscale domains offers a promising way to engineer the properties and to achieve optimal performances.

Besides HNCs, hollow/porous magnetic NCs have been increasingly investigated in recent years.[36–40] The hollow interiors and porous shells within the NCs can provide high surface to volume ratio and large pore volume, which are highly attractive for many technological applications. For example, drugs that are initially encapsulated in the void part of the hollow NC can be released either chemically via a pH control or physically through a magnetic stimulation and photothermal activation, offering a new approach for simultaneous diagnostic and therapeutic applications.[41–43]

Compared to the top–down physical processes, colloidal chemical synthetic methods have been found to be highly effective to synthesize uniform magnetic NCs with controlled

*Project supported by the National Basic Research Program of China (Grant No. 2010CB934601), the National Natural Science Foundation of China (Grant Nos. 51125001, 51172005, and 90922033), the Natural Science Foundation of Beijing (Grant No. 2122022), the Doctoral Program Foundation (Grant No. 20120001110078), the New Century Talent Foundation of the Education Ministry of China (Grant No. NCET-09-0177), the Yok Ying Tung Foundation (Grant No. 122043), and the PKU COE-Health Science Center Seed Fund.

†Corresponding author. E-mail: hou@pku.edu.cn

© 2013 Chinese Physical Society and IOP Publishing Ltd

sizes and shapes by varying the reaction conditions.[44,45] In this review, we present recent advances in the chemical synthesis of various types of magnetic NCs. General synthesis of single-component magnetic NCs, multi-component magnetic NCs (including core/shell heterostructure, oligomer-like heterostructure, and anisotropically shaped material-based heterostructure), and hollow/porous magnetic NCs are summarized.

2. Chemical synthesis of single-component magnetic NCs

To prepare magnetic NCs with controlled sizes and shapes, various methods based on solution-phase colloidal chemistry have been intensively investigated.[46–54] Among them, thermal decomposition and/or reduction approach is one of the most attractive techniques which can meet the requirement of preparing high quality magnetic NCs. In this section, we focus on some recent developments related to the colloidal chemical synthesis of magnetic NCs from metal oxides, metals, alloys, metal carbides, phosphides, and chalcogenides.

2.1. Metal oxides

Magnetic metal oxide NCs such as iron oxides are very important for various biological applications, such as MRI, drug delivery, cell tracking, protein separation, and hyperthermia.[55–57] FeO, γ-Fe_2O_3, and Fe_3O_4, which possess remarkably different magnetic properties, are three typical phases of iron oxides. Co-precipitation of Fe^{3+} and Fe^{2+} salts in a basic solution is the simplest method for synthesizing iron oxide NCs.[58–62] Despite the ease and large-scale producibility of this approach, it is difficult to prepare the NCs with narrow size distribution, high crystallinity, and high magnetization values. Thermal decomposition reaction of an iron precursor in a high-boiling-point organic solvent offers a promising way to synthesize highly monodisperse iron oxide NCs. For example, Sun *et al.* obtained monodisperse Fe_3O_4 NCs with a size range of 4 nm–20 nm by reductive decomposition of iron (III) acetylacetonate ($Fe(acac)_3$, acac = acetylacetonate) in the mixture of 1,2-hexadecanediol, oleic acid (OA), oleylamine (OAm), and benzyl ether (Fig. 1).[63] It was found that the type of solvent and reaction temperature could determine the size of Fe_3O_4 NCs. Additionally, via seed-mediated growth, larger NCs with the size of 20 nm could be produced (Fig. 1(b)). Hyeon *et al.* developed an ultra-large-scale synthetic method to prepare monodisperse iron oxide NCs using iron–oleate complex as the precursor, which can be prepared by the reaction of inexpensive and nontoxic iron chloride with sodium oleate.[64] By slowly heating the mixture of Fe-oleate complex and surfactant to the boiling point (bp) of the solvent, monodisperse iron oxide NCs were produced. The size of the iron oxide NCs could be easily controlled by varying the solvent with different bp. 5-nm, 9-nm, 12-nm, 16-nm, and 22-nm iron oxide NCs were prepared using 1-hexadecene [bp: 274 °C], octyl ether (bp: 287 °C), 1-octadecene (bp: 317 °C), 1-eicosene (bp: 330 °C), and trioctylamine (bp: 365 °C) as solvent, respectively. Cube-shaped Fe_3O_4 NCs in the size range from 20 nm to 160 nm could be synthesized by thermal decomposition of $Fe(acac)_3$ in the presence of OA and benzyl ether at 290 °C.[65] Very recently, Hyeon *et al.* reported the preparation of uniform and extremely small iron oxide NCs of less than 4 nm via the thermal decomposition of an iron–oleate complex in the presence of oleyl alcohol.[66] The formation of extremely small iron oxide NCs was ascribed to oleyl alcohol which could lower the reaction temperature by reducing iron–oleate complex. Moreover, by tuning the ratio of oleyl alcohol to OA or changing the temperature, Fe_3O_4 NCs could be controlled in the size range from 1.5 nm to 7 nm. The wüstite-type FeO NCs were also prepared via thermal reductive decomposition reactions. Hou *et al.* synthesized size- and shape-controlled FeO NCs by reductive decomposition of $Fe(acac)_3$ in the mixture of OA and OAm (Fig. 2).[67] The size of the FeO NCs was controlled in the range of 14 nm–100 nm and the shapes were either polyhedra or truncated octahedra by varying the molar ratio of OA to OAm. It is worth noting that other types of iron oxide (Fe_3O_4, γ-Fe_2O_3, or γ-Fe_2O_3 NCs) could be obtained from the as-synthesized FeO NCs under controlled annealing conditions.

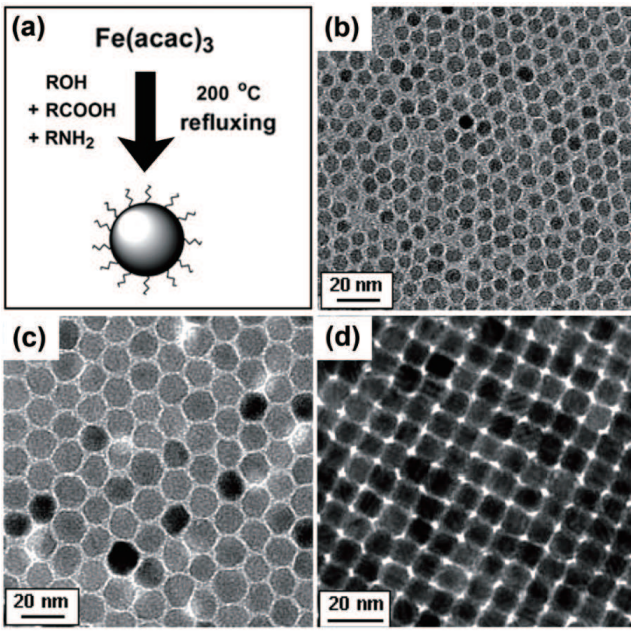


Fig. 1. (a) Schematic illustration of the synthesis of monodisperse Fe_3O_4 NCs through the decomposition of $Fe(acac)_3$ in the presence of oleic acid, oleylamine, and alkanediol. Transmission electron microscopy (TEM) image of (b) 6-nm and (c) 10-nm Fe_3O_4 NCs. (d) A three-dimensional (3D) superlattice of 10-nm Fe_3O_4 NCs. Reproduced with permission from Ref. [63]. Copyright 2004 American Chemical Society.

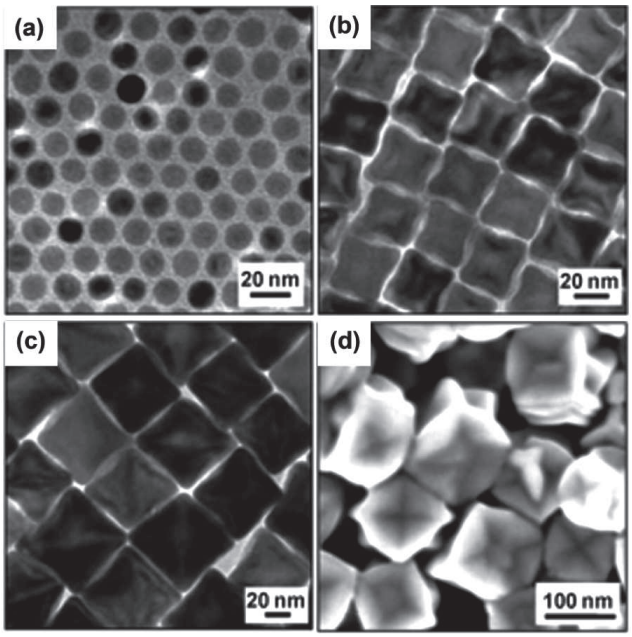


Fig. 2. TEM images of FeO NCs with different sizes and shapes: (a) 14-nm spherical, (b) 32-nm, and (c) 53-nm truncated octahedral. (d) Scanning electron microscopy (SEM) image of 100-nm truncated octahedral NCs. Reproduced with permission from Ref. [67]. Copyright 2007 Wiley-VCH.

Ferrite $M\text{Fe}_2\text{O}_4$ NCs generated from the partial substitution of Fe^{2+} with other transition metal M^{2+} (M = Mn, Co, Ni, Zn, etc.) in the crystal lattice of magnetite (Fe_3O_4) have also attracted much attention for their distinct magnetic properties induced by M-doping compared to Fe_3O_4.[68] The approach to the synthesis of monodisperse $M\text{Fe}_2\text{O}_4$ NCs is similar to that of Fe_3O_4 NCs discussed above. Typically, to prepare monodisperse CoFe_2O_4 or MnFe_2O_4 NCs, a stoichiometric amount of $M(\text{acac})_2$ (M = Co, Mn) and Fe(acac)_3 were mixed and heated in a high-boiling-point solvent in the presence of OA and OAm (Figs. 3(a) and 3(b)).[63] The size of the NCs can be tuned from 3 nm to 20 nm by varying reaction conditions such as temperature and types of precursors or by seed-mediated growth. Alternatively, Hyeon *et al.* fabricated spinel $M\text{Fe}_2\text{O}_4$ NCs (M = Mn, Co or Ni) by means of a high-temperature, nonhydrolytic reaction between divalent metal chloride and Fe(acac)_3 in the presence of OA and OAm as surfactants.[69] Cheon *et al.* synthesized a series of 15-nm sized Zn^{2+}-doped NCs of $(\text{Zn}_x\text{Mn}_{1-x})\text{Fe}_2\text{O}_4$ and $(\text{Zn}_x\text{Fe}_{1-x})\text{Fe}_2\text{O}_4$ ($x = 0$, 0.1, 0.2, 0.3, 0.4, and 0.8) with single crystallinity and size monodispersity by thermal decomposition of metal chloride precursors and Fe(acac)_3 in the solution of OA, OAm, and octyl ether (Figs. 3(c) and 3(d)).[70] The Zn^{2+} doping level, which was carefully controlled by varying the initial molar ratio of the metal chloride precursors, determined the magnetic properties of the ferrite NCs. For example, the saturation magnetization of $(\text{Zn}_x\text{Mn}_{1-x})\text{Fe}_2\text{O}_4$ NCs ($x = 0$, 0.1, 0.2, 0.3, and 0.4) was found to be 125, 140, 154, 166, and 175 emu·g^{-1} (metal atoms), respectively. Recently, the same group improved the synthetic method for realizing size- and shape-controlled synthesis of zinc ferrite NCs.[71] 22-nm spherical $\text{Zn}_{0.4}\text{Fe}_{2.6}\text{O}_4$ NCs were obtained by the reaction of Fe(acac)_3 and zinc chloride in the presence of OA, OAm, and octyl ether at 330 °C. To prepare cube-shaped NCs, the precursors were heated in the presence of OA and benzyl ether. By changing the concentration of Fe(acac)_3 and zinc chloride, the size of the NCs could be conveniently tailored from 18 nm to 140 nm.

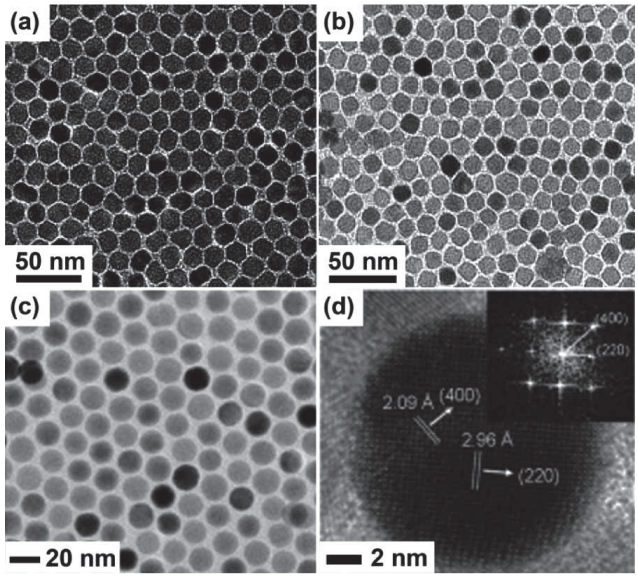


Fig. 3. TEM images of 14-nm (a) CoFe_2O_4 NCs and (b) MnFe_2O_4 NCs. Reproduced with permission from Ref. [63]. Copyright 2004 American Chemical Society. (c) TEM image and (d) high-resolution TEM (HRTEM) image of 15-nm $(\text{Zn}_{0.4}\text{Fe}_{0.6})\ \text{Fe}_2\text{O}_4$ NCs. Reproduced with permission from Ref. [70]. Copyright 2009 Wiley-VCH.

2.2. Metals and alloys

Metallic Fe, Co, Ni are typical classes of ferromagnetic (FM) materials with high saturation magnetization. Among them, iron possesses the highest room-temperature value of saturation magnetization, and has a Curie temperature (T_c) that is high enough for practical applications.[72–74] Therefore, iron NCs have attracted a great deal of interest in sensitive MRI and magnetic fluid hyperthermia applications. However, metallic Fe NCs are very reactive and unstable, specifically with respect to water and oxygen, and can be rapidly and completely oxidized in air to form various iron oxide NCs with much reduced magnetizations. Recently, researchers are challenging in the synthesis of metallic Fe NCs that can be stabilized against fast oxidation.[75–78] The two well-known approaches to monodisperse Fe NCs are the thermal decomposition and chemical reduction of an iron organocomplex. Iron pentacarbonyl, Fe(CO)_5, is generally used to produce Fe NCs via decomposition in organic solutions. In a typical process, monodisperse Fe NCs were prepared by thermal decomposition of Fe(CO)_5 in 1-octadeceneand OAm at 180 °C.[79] To increase the chemical and dispersion stability of the NCs, a crystalline Fe_3O_4 shell was created over the core by controlled

oxidation of the iron surface via the oxidant $(CH_3)_3NO$. Interestingly, it was found that the addition of hexadecylamonium chloride could yield body centered cubic Fe NCs with drastically increased magnetization (Fig. 4(a)).[78] Concerning the chemical reduction, the complex $Fe[N(SiMe_3)_2]_2(THF)$ (Me = CH_3, THF=tetrahydrofuran) and $Fe[N(SiMe_3)_2]_2$ have been chosen as iron sources to produce metallic Fe NCs. Dumestre *et al.* reported the reaction of $Fe[N(SiMe_3)_2]_2$ with H_2 in the presence of hexadecylamine (HDA) and OA to prepare monodisperse zerovalent iron NCs with controlled sizes (Fig. 4(b)).[77] It is worth noting that the magnetizations of the as-prepared NCs were found close to bulk values. In an improved procedure that argon was used as atmosphere instead of H_2, the reaction of $Fe[N(SiMe_3)_2]_2$ was held to yield single-crystalline iron NCs of uniform size and shape with the assistance of ammonium chloride HDA·HCl.[75] Alternatively, by the reduction of the iron–oleate complex at a high temperature of 380 °C in the mixture of OA and 1-octadecene, cube-shaped 20-nm iron NCs which is passivated by a thin FeO layer were produced.[64]

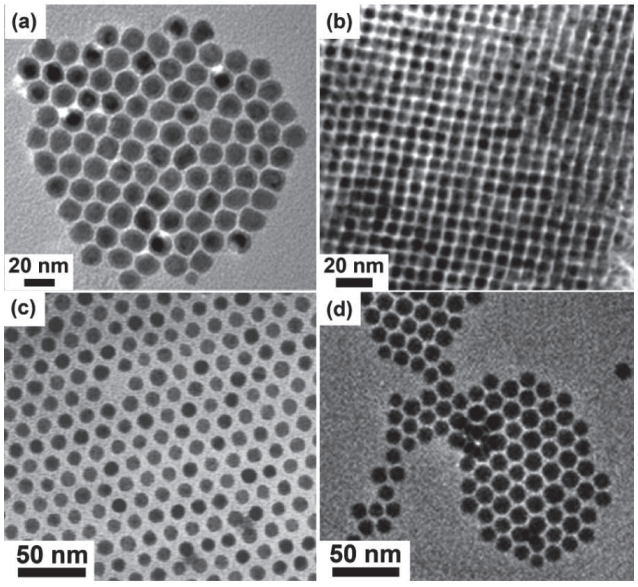


Fig. 4. (a) TEM image of the 15-nm Fe NCs. Reproduced with permission from Ref. [78]. Copyright 2011 American Chemical Society. (b) TEM image of 3D superlattice of Fe nanocubes. Reproduced with permission from Ref. [77]. Copyright 2011 Science. (c) TEM image of a two-dimensional (2D) assembly of 9-nm Co NCs. Reproduced with permission from Ref. [84]. Copyright 1999 American Institute of Physics. (d) TEM image of Ni NCs with the size of 12.8±0.7 nm. Reproduced with permission from Ref. [90]. Copyright 2009 American Chemical Society.

Similar as iron, the preparation of cobalt NCs is via thermal decomposition or chemical reduction of organometallic precursors. However, Co atoms can crystallize into three types of phases including hexagonal close packed (hcp), face-centered cubic (fcc), or ε-phase with distinct magnetic properties.[80–86] By varying precursors, surfactant species, and/or reaction temperatures, the size and shape for Co NCs can be efficiently controlled. To synthesize ε-Co NCs, a very sensitive phase to the reaction conditions, Sun *et al.* reported the reduction of cobalt chloride using lithium triethylborohydride ($LiBEt_3H$, superhydride) in dioctyl ether with OA and trialkylphosphine as the capping agents (Fig. 4(c)).[84] The increase of the reaction temperature from 200 °C to 300 °C would yield hcp-Co NCs. Besides, the group of Alivisatos developed a method by employing cobalt carbonyl as the precursor, from which monodispersed, stabilized, defect-free ε-cobalt NCs, with spherical shapes and sizes ranging from 3 nm to 17 nm could be produced.[87] Cobalt NCs in the hcp and fcc phase could also be synthesized. Monodisperse hcp-Co NCs could be prepared from cobalt acetate solution in diphenyl ether using a mild reducing reagent (1,2-dodecanediol) at 240 °C in the presence of OA and n-trioctylphosphine (TOP). By adjusting the capping groups/metal salt ratio and selecting the degree of bulkiness of the organophosphine stabilizer, the size of Co NCs could be further tuned.[88] Puntes *et al.* acquired hcp-Co disk-shaped NCs by rapid decomposition of cobalt carbonyl in the presence of linear amines.[89] As selective adsorption of alkylamine might inhibit growth along a unique axis, disk-shaped NCs were formed. The decomposition of $Co_2(CO)_8$ in the presence of stabilizing ligands could also yield multiply twinned fcc-Co NCs with narrow size distributions. Typically, to prepare 8- to 10-nm fcc-Co NCs, $Co_2(CO)_8$ dissolved in dioctyl ether was injected into the mixture of diphenyl ether/OA/tributylphosphine at 200 °C.[88]

Besides Fe and Co, the synthesis of Ni NCs have also been intensively investigated. Based on the chemical reduction of nickel salts $Ni(CH_3COO)_2$ or $Ni(acac)_2$ in the presence of the ligands (OA, TOP or OAm), monodisperse Ni colloidal NCs in the 4 nm–16 nm size range with narrow size distribution were successfully produced (Fig. 4(d)).[90] By controlling the synthetic conditions (precursors, ligands and temperature), the size of Ni NCs could be easily tuned. Zhang *et al.* employed three processes, including direct thermolysis, seed-assisted growth, and hot injection, to synthesize Ni NCs with diameters in the range of 20 nm–60 nm by the decomposition of nickel acetylacetone in OAm.[91] Cordente *et al.* synthesized nickel NCs of tunable shape from the decomposition of $Ni(COD)_2$ (COD = cycloocta-1,5-diene) in THF in the presence of HDA or trioctylphosphine oxide (TOPO).[92] By increasing the concentration of amine, nearly monodisperse Ni nanorods were formed probably due to the specific coordination of the amine. On the other hand, monodisperse Ni NCs could also be prepared at low temperature with the help of strong reductants. Metin *et al.* fabricated monodisperse Ni NCs (≈ 3 nm) from the reduction of $Ni(acac)_2$ with the strong reducing agent boranetributylamine (BTB) in OAm and OA. In principle, the crystalline structure of the Ni NCs, which are generated from the thermal reduction of Ni salts in

alkylamines, can be tuned by adjusting the reaction temperature. Chen *et al.* observed the formation of hcp-Ni NCs at higher reaction temperatures (e.g., > 240 °C) from the reduction of $Ni(acac)_2$ in alkylamines.[93] On the other hand, lower temperatures yielded fcc-Ni NCs. Mourdikoudis *et al.* reported a similar phase change of Ni NCs based on the thermal decomposition of nickel acetate tetrahydratein primary and tertiaryamines[94] Ni nanostructures with either hcp or fcc crystal structure could be tuned by the reaction temperature, and the size of the particles could be controlled between 5 nm and 120 nm by the additional surfactants such as 1-adamantanecarboxylic acid (ACA).

The synthesis of nanostructured alloys such as FePt and CoPt have also been intensively studied because of their high magneto-anisotropy and good chemical stability.[1,95,96] Nanostructured MPt alloys with the phase of face-centered tetragonal (fct) (also known as $L1_0$ phase) are particularly interesting for their extremely high magneto-anisotropy which makes them excellent candidates for ultrahigh-density magnetic storage and the precursor to advanced magnetic materials. Sun *et al.* first obtained monodisperse FePt NCs by the thermal decomposition of $Fe(CO)_5$ and the reduction of $Pt(acac)_2$ in a mixture of OA and OAm (Fig. 5).[1] The size and composition of FePt NCs could be tuned by varying the ratio of precursors and the solvent. Exclusion of additional reducing agent such as 1,2-alkanediol in the reaction mixture can help realize better control of the size of the FePt NCs.[97,98] To convert as-synthesized FePt NCs with a chemically disordered fcc structure into an fct structure, thermal annealing of fcc-FePt NCs at high temperatures is needed. To obtain dispersible fct-FePt NCs, one can coat the as-synthesized FePt NCs with SiO_2/MgO, or disperse the NCs in NaCl matrix before thermal annealing, and remove the additional chemicals after the fct-FePt is formed.[69,99–103] Notably, the direct synthesis of fct-FePt NCs using a wet-chemistry method was also reported. Jeyadevan *et al.* obtained partial fct-FePt alloys with a particle size of 5 nm–10 nm by the reduction of platinum and iron acetylacetonates in tetraethylene glycol at 300 °C.[104] Howard *et al.* acquired partially ordered fct-FePt NCs by the reaction of $Na_2Fe(CO)_4$ and $Pt(acac)_2$ in tetracosane at 389 °C.[105] Owing to the unique magnetic properties including large permeability and very high saturation magnetization, FeCo alloys are very attractive for self-assembly thin film and biomedical applications. Based on reductive decomposition of $Fe(acac)_3$ and $Co(acac)_2$ in a mixture of OA, OAm, and 1,2-hexadecanediol under a gas mixture of 93% Ar + 7% H_2 at 300 °C, Chaubey *et al.* successfully obtained bimetallic FeCo NCs with well-controlled particle size and size distribution.[106] By using $[Co(\eta^3\text{-}C_8H_{13})(\eta^4\text{-}C_8H_{12})]$ and $Fe(CO)_5$ as organometallic precursors and a mixture of HDA, OA, and stearic acid (SA) as stabilizing agents at 150 °C under 3 bars (1 bar = 10^5 Pa) of H_2, 20-nm monodisperse FeCo NCs, self-organized into millimeter long supercrystals, could be obtained.[107] In an alternative approach, high-magnetic-moment FeCo NCs were prepared via the diffusion of Co and Fe in core/shell structured Co/Fe NCs by raising the solution temperature.[108]

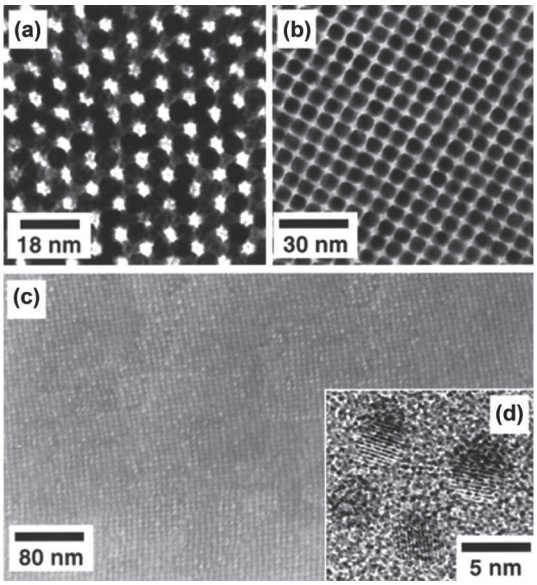


Fig. 5. (a) and (b) TEM image of a 3D assembly of 6-nm $Fe_{50}Pt_{50}$ NC. (c) High-resolution SEM image and (d) HRTEM image of 4-nm $Fe_{52}Pt_{48}$ assembly after annealing. Reproduced with permission from Ref. [1]. Copyright 2000 Science.

2.3. Metal carbides, phosphides, and chalcogenides

Nanosized iron carbides have attracted increasing interest recently due to their good air stability with high magnetization, and excellent catalytic properties in the Fischer–Tropsch synthesis.[109,110] However, to meet the requirements of wide applications, there still remain big challenges in the synthesis of iron carbide nanostructures with controlled phase, size, and magnetic properties. Compared to the preparation routes of physical pyrolysis, sonolysis, and laser ablation methods, which inevitably cause the aggregation of products, solution chemistry methods have shown remarkable advantages in controlling the size and morphology.[111–115] Hou *et al.* developed a convenient solution phase method to synthesize Fe_5C_2 NCs by the reaction of $Fe(CO)_5$ with octadecylamine in the presence of bromide under mild temperatures.[114] It was investigated that bromide in the reaction systems was crucial for the formation of crystalline Fe NCs, which exhibited antioxidized characteristics to proceed to carbonization at high temperature. On the other hand, unsaturated hydrocarbons and cyanides, which were produced by the decomposition of octadecylamine under Fe catalysis, served as carbon source that could react with crystalline Fe to form Fe_5C_2. Owing to the compact organic shell around the NCs built by bulky octadecylamine, the size of the carbide could be effectively controlled. Inspired by the Fischer–Tropsch process, Meffre *et al.* reported a tunable

organometallic synthesis of monodisperse iron carbide NCs based on the decomposition of $Fe(CO)_5$, which serves as both Fe and carbon precursor, in the presence of preformed Fe NCs at 150 °C under 3-bar H_2 atmosphere.[115] By carefully altering the surface functional groups of preformed Fe seeds, solvent and $Fe(CO)_5$ concentration, iron carbide NCs with a very narrow size distribution could be obtained (Fig. 6(a)). Because of their excellent magnetic properties with tunable magnetic anisotropy, these NCs displayed extremely high efficiency for magnetic hyperthermia.

There have been some reports on chemical synthesis of cobalt carbide NCs with interesting magnetic properties. The polyol, which can effectively reduce cobalt salts and generate active carbon, has been exploited to fabricate cobalt carbide NCs.[116–118] Zhang *et al.* reported the controlled synthesis of cobalt carbide (Co_3C and Co_2C) NCs with high coercivity at room temperature based on a simple one-pot polyol reduction process, in which the shape and size of the cobalt carbide NCs could be controlled by adjusting the category and concentration of the surfactant.[118] The polyol reduction method could be further improved with the help of hydroxide and chloride anions, which could affect the size and phase of cobalt carbide.[117] It is interesting that by varying the concentration of the anions, pure phase Co_2C NCs were prepared. In an alternative process, An *et al.* performed the reduction of the self-assembled CoO nanorod arrays to form FM Co_2C nanorods arrays.[119] Under H_2 atmosphere, CoO was initially reduced to form Co, and reacted with the carbon from the thermal decomposition of the organic surfactant. In spite of the preliminary progress, to develop a reliable method to synthesize high-quality cobalt carbide NCs with pure phase and homogeneous size is still highly desired for practical applications.

Based on the reactions carried out in high-boiling-point organic solvents, there have been many efforts in synthesizing colloid nickel carbide NCs.[120,121] Pure nickel carbide (Ni_3C) NCs, which is characterized as an interstitial solid solution of carbon in the metallic hcp-Ni, have been prepared with particle diameters of 40 nm by thermal decomposition of nickel formate in the presence of OA and OAm. However, due to similar lattice parameters between hcp-Ni and Ni_3C, there remains controversy in examination of the exact phase. Goto *et al.* demonstrated the thermolysis of $Ni(acac)_2$ in OAm to acquire Ni_3C NCs, and used hard-X-ray photoelectron spectroscopy to clarify that the hcp phase was not a metallic hcp-Ni but a hexagonal nickel carbide.[120] During the process, metallic Ni NCs were first generated by the thermal decomposition of the acetylacetonate, and then were subjected to carbonization to form cubic nickel carbide as an intermediate product before being transformed into hexagonal nickel carbide. By decomposing $Ni(acac)_2$ in the presence of OAm and 1-octadecene, Schaefer *et al.* synthesized Ni_3C_{1-x} with controlled average carbon content via tuning the reaction time.[121] Their results help to experimentally rationalize the discrepancies in lattice constants and magnetic properties, and effectively bridge prior reports of hcp-Ni and Ni_3C.

Magnetic metal phosphides including iron, cobalt, and nickel phosphides, are a class of compounds that have gained increasing interest for their advanced catalytic, electronic, and magnetic properties.[122,123] Recent studies have been focused to develop general synthetic approaches to synthesize high crystalline magnetic metal phosphides with careful control over both the composition and the morphology.[124–135] In general, the preparation of metal phosphides is based on the reaction between phosphorus containing chemicals (phosphines, phosphorus pentachloride, $P(SiMe_3)_3$ or trictylphosphine) and metal precursors. Perera *et al.* first reported the preparation of pure FeP NCs from reaction of $Fe(acac)_3$ with $P(SiMe_3)_3$ in TOPO at 280 °C.[136] Instead of $P(SiMe_3)_3$, the use of alkyl phosphines, like TOP, as the phosphorus source has proven to be a more general and cheaper route to synthesize magnetic metal phosphide NCs. Henkes *et al.* described a general strategy for synthesizing various types of transition metal phosphides nanostructures by the conversion of preformed metal NCs into metal phosphides via solution-mediated reaction with TOP.[132] Similarly, the Brock group reported the synthesis of phase-pure Fe_2P and FeP by reacting preformed Fe NCs with TOP at temperatures in the region of 350 °C–385 °C. It was found that shorter reaction time/lower temperature favored an iron-rich product (Fe_2P), and longer reaction time/higher temperature favored a phosphorus-rich product (FeP).[124] Ha *et al.* reported the chemical transformation of ε-Co NC into two phases of cobalt phosphide, Co_2P, and CoP from a reaction with TOP.[130] Discrete, unsupported NCs of Ni_2P with an average crystallite size of 10.2 ± 0.7 nm have been prepared by using a solution-phase method with $Ni(COD)_2$ as the nickel source and TOP as the phosphorus source in the presence of the coordinating solvent TOPO.[126] Muthuswamy *et al.* presented controlled synthetic procedures to utilize reaction parameters as levers to tune phase, size, and morphology, enabling phase-pure samples of $Ni_{12}P_5$ and Ni_2P to be prepared in both solid and hollow morphologies.[125] In order to get anisotropic nanostructures of the metal phosphides, Liu[134] and Hyeon[137] developed the method to promote the growth of anisotropic NCs by multiple or continuous injection of a metal-TOP precursor solution. For example, well-defined FeP nanorods and nanowires were acquired by the multiple injection of iron pentacarbonyl and phosphine mixtures (Fig. 6(b)),[134] while uniformly sized magnetic Fe_2P nanorods could be fabricated from the thermal decomposition of continuously delivered iron-phosphine complex using a syringe pump. By controlling the injection rate and by using different surfactants, the diameters and aspect ratios of the

nanorods could be conveniently controlled, thus MnP, Co_2P, FeP, NiP nanorods with various dimensions could be successfully obtained (Fig. 6(c)).[133] In an alternative process without continuous injection, Li *et al.* employed a simple and reproducible method to prepare CoP nanowires with a high aspect by the thermal decomposition of $Co(acac)_2$ and tetradecyl phosphonic acid in a mixture of TOPO and HDA. Zhang *et al.* presented the use of TOPO, an air-stable compound, as both a solvent and a controlled phosphorus source to produce hyperbranched Co_2P NCs that are uniform in size, shape, and symmetry (Fig. 6(d)).[135]

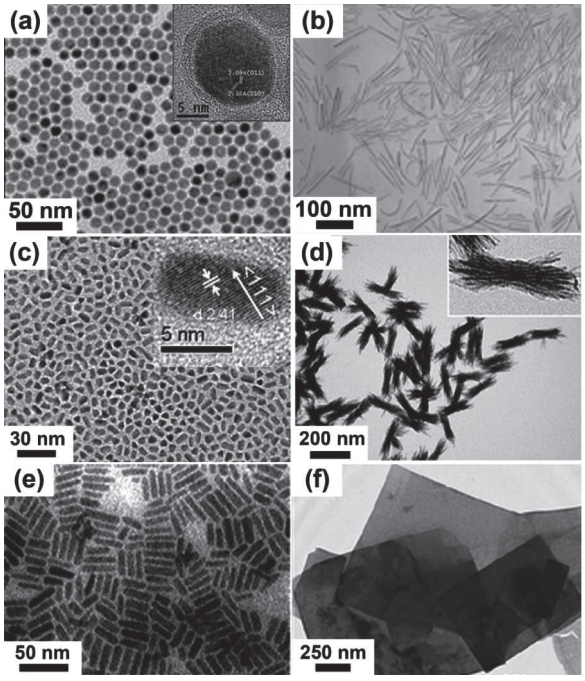


Fig. 6. TEM image of (a) 13.1-nm iron carbide NCs, (b) FeP nanowires, (c) Ni_2P nanorods, (d) hyperbranched Co_2P NCs, (e) NiS nanorods, and (f) β-FeSe nanosheets. Reproduced with permission from Refs. [115], [133]–[135], [140], and [141], respectively. Copyright 2012, 2004, 2005, 2011, 2004, 2009 American Chemical Society.

Magnetic metal chalcogenides are also an important family of interesting materials that have been proven to possess great potentials in many fields due to their magnetic, electrochemical, optical, and electrical properties. By taking advantages of solution-based chemical route, many groups have been challenging the syntheses of magnetic metal chalcogenides with tunable sizes and variable shapes. Notably, from previous studies, the hot-injection method and single-source precursor method have been proved to be highly effective strategies for preparing magnetic metal chalcogenides nanostructures. By employing a single source precursor, $[N^nBu_4]_2[Fe_4S_4(SPh)_4]$, bis(tetra-n-butylammonium)tetrakis[benezenethiolato-μ_3-sulfido-iron], a cubane-type cluster, which can decompose under extended reflux in alkylamines, O'Brien and Vanitha prepared monodispersed superparamagnetic iron sulfide NCs with controlled composition, structure, and dimensions.[138] In the procedures, pyrrhotite type Fe_7S_8 NCs were formed at 180 °C, while Fe_3S_4 with a greigite structure was obtained at a higher temperature of 200 °C. In another approach, by decomposing a single-source precursor of $Fe(Ddtc)_3$ or $Fe(Ddtc)_2(Phen)$ (Phen = 1,10-phenanthroline; Ddtc = diethyldithiocarbamate) in the mixture solvents of OA/OAm/1-octadecene, Fe_3S_4 and Fe_7S_8 nanostructures displaying strong FM properties at room temperature have been synthesized with diverse shapes (NCs, nanoribbons and nanoplates).[139] By extending the single source precursor method, rhombohedral NiS (millerite) nanorods and triangular nanoprisms could be synthesized relied on the thermal degradation of nickel thiolate precursors in the presence of octanoate.[140] Owing to solventless environment where interparticle collisions are rare, and controlled growth process, NiS NCs are achieved with relatively homogeneous size and shape (Fig. 6(e)). Raymond E. Schaak and his colleagues made an important contribution in the synthesis of iron chalcogenide via solution chemistry, where by β-FeSe, Te-containing compounds and the composition-tunable β-Fe(Se, Te) solid solution could be acquired by adopting $Fe(CO)_5$ as an iron source and TOPO as solvent (Fig. 6(f)).[141] Bi *et al.* obtained phase pure, highly crystalline cubic FeS_2 NCs by using a TOPO assisted hot-injection method.[142] Chen *et al.* prepared uniform tetragonal b-$FeSe_x$ square nanoflakes with tunable composition and size by the reaction between ferrous chloride and selenium trioctylphosphine in the presence of OAm and OA.[143] Very recently, one-step colloidal synthetic methods have attracted increasing attention due to the avoidance of complicated procedures and harsh synthetic conditions. In a representative process, Zhang *et al.* have developed a convenient protocol for synthesizing Fe_3Se_4 nanostructures (nanosheets, nanocacti, and nanoplatelets) by the one-pot high temperature organic-solution-phase method.[144] Interestingly, the as-synthesized Fe_3Se_4 nanostructures exhibit hard magnetic properties, with giant coercivity values up to 40 kOe (1 Oe = 79.5775 $A{\cdot}m^{-1}$) at 10 K and 4 kOe at room temperature.

3. Chemical synthesis of multi-component magnetic NCs

HNCs, which are composed of different inorganic components with various types of interfaces, have recently attracted much attention due to the unique properties and numerous possibilities of applications.[20–22,26–30] In terms of multi-component magnetic nanostructures, the different domains meet at interfaces open an opportunity to adjust the magnetism. In addition, the functional components involved in individual magnetic nanostructures may provide a platform for recyclable catalysis, medical diagnosis and therapy, photonics and electronics.[27,29,32,145] In order to realize the suc-

cessful application of such nanocomposites, it is extremely important to control their nanostructure, composition, and stability under different conditions. Therefore, in the past years many researchers have devoted themselves to developing reliable synthetic methods to fabricate the magnetic multi-component nanostructures. Among those approaches, non-hydrolytic method was found to be one of the most efficient and controllable ways to obtain the required NCs. In this part, we briefly overview the recent advances in the nonhydrolytic chemical synthesis of magnetic multi-component NCs with different nanostructures including core/shell, oligomer-like and anisotropically shaped material-based heterostructure.

3.1. Core/shell heterostructure

In the systems of core/shell nanostructures, the inorganic inner NC "core" is evenly covered with a shell coating, which may be composed of one or more layer of inorganic materials. The magnetism of core and/or shell contributes to the magnetic property of the whole structure. Due to the large area of interfaces and related strong interactions, the physico–chemical properties of the core/shell nanostructures are found to be quite distinct from the individual components. In terms of magnetic NCs, the interactions at the interface always lead to the variation of the magnetism, such as the exchange bias effect and exchange-coupling-caused increase of magnetic energy product.[146–150]

In order to successfully obtain the core/shell nanostructures, epitaxial growth is worth consideration. When the core and shell components are characterized by similar crystal structure and/or close matching lattice space, the strain at the interfaces can be minimized, resulting in the formation of core/shell structures, otherwise islands or satellites would finally appear for the decrease of the interface energy. However, the lattice compatibility is not necessary to achieve core/shell nanostructures. For example, the uniform oxidation of the active core NCs is an effective strategy to establish core/shell geometry.

Zeng *et al.* first synthesized bimagnetic FePt/Fe_3O_4 core/shell NCs by reductive decomposition of $Fe(acac)_3$ in the presence of monodisperse FePt NCs (Fig. 7(a)).[151] The seed-mediated approach was found to be effective for the uniform growth of iron oxide. By adjusting the molar ratio between FePt NCs and the $Fe(acac)_3$ precursor, the shell thickness could be easily tuned. Similarly, magnetic $CoFe_2O_4$ shell could also be achieved by introducing $Co(acac)_2$ into the system.[146] Besides FePt NCs, other metal/alloy NCs could also be used as seeds to generate metal/iron oxide core/shell nanostructures. It was suggested that metal/alloy seeds were generally rich of electrons, which could serve as catalytic centers for the growth of the secondary component. Shi *et al.* synthesized monodisperse Au/Fe_3O_4 core/shell NCs with epitaxial interfaces by decomposing $Fe(CO)_5$ or $Fe(acac)_3$ in the presence of small Au seeds (Fig. 7(b)).[152] Co/Sm_2O_3 core/shell NCs (Fig. 7(c)) obtained from solution phase processing were used as precursors for high-temperature annealing, yielding nanocrystalline $SmCo_5$ with large coercivity.[153] Teng *et al.* reported the synthesis of Pt/Fe_2O_3 core/shell NCs by sequential decomposition of $Pt(acac)_2$ and $Fe(CO)_5$ (Fig. 7(d)).[154] FePt/ZnO core/shell NCs could be prepared by the decomposition of zinc acetate at high temperature in the presence of uniform FePt seeds, which offered a good example to combine the magnetism and fluorescence.[155]

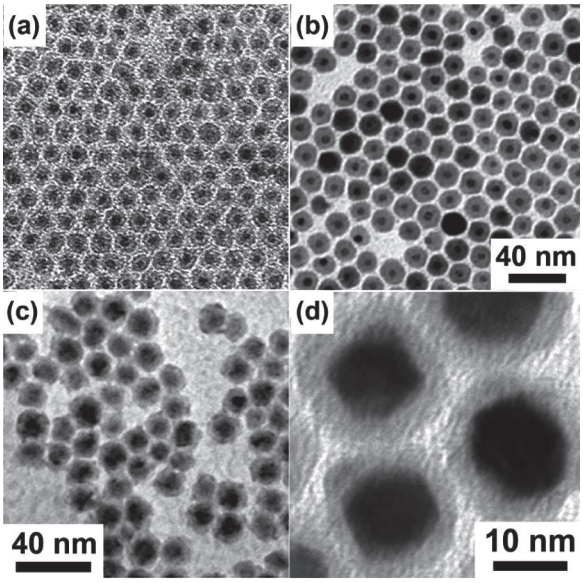


Fig. 7. TEM images of typical metal/oxide core/shell HNCs prepared by seed-mediated process. (a) FePt/Fe_3O_4 core/shell HNCs. Reproduced with permission from Ref. [151]. Copyright 2004 American Institute of Physics. (b) Au/Fe_3O_4 core/shell HNCs. Reproduced with permission from Ref. [152]. Copyright 2006 American Chemical Society. (c) Co/Sm_2O_3 core/shell HNCs. Reproduced with permission from Ref. [153]. Copyright 2007 Wiley-VCH. (d) Pt/Fe_2O_3 core/shell HNCs. Reproduced with permission from Ref. [154]. Copyright 2003 American Chemical Society.

All-oxides magnetic NCs are also important series of core/shell NCs for wide application potentials. The spinel-phase MFe_2O_4 (M = Zn, Mn, Fe, Co, Ni) are those types of ferrimagnetic (FiM) materials which deserve to be mentioned. The incorporation of both FM (or FiM) and antiferromagnetic (AFM) phase in the core/shell structure brings the signature of magnetic exchange coupling between interfacial spins of the two types of magnetic sections, which may cause horizontal loop shift by an "exchange bias" field, thus resulting in enhancement of the coercivity.[148,149,156] In addition, effective interfacial exchange interaction also occurs between soft and hard magnetic phases if the thickness of soft phase is twice the width of domain wall of the hard phase. In this case, soft phase becomes rigidly pinned by hard phase at the interface.[71,99,146,150] This unique effect offers opportunities to tune the magnetism of the NCs and therefore to realize ideal

performances. The preparation of all spinel phase core/shell NCs are generally easy to carry out due to the similar crystal structures and lattice spaces between the components. Uniform core/shell NCs incorporating all magnetic spinel phase can be obtained with controlled size and shell thickness based on the seeds-mediated process. For instance, to synthesize 15-nm core/shell $CoFe_2O_4/MnFe_2O_4$ NCs, a 9-nm $CoFe_2O_4$ NC was used as a seed and $MnFe_2O_4$ was over-grown onto the surface of the seed particle by thermal decomposition of the $MnCl_2$ and $Fe(acac)_3$.[99] By tuning the amount of the precursors, the shell thickness of the secondary component could be easily controlled. The AFM phase of MnO could be overgrown onto the spinel ferrite by decomposition of $Mn(CH_3CO)_2$ via similar seed-mediated method, which generated the FM/AFM interactions at the core/shell interfaces.[157]

Another smart family of core/shell NCs, in which the FM (or FiM) core, such as FePt, Fe_3O_4, was covered by the noble metal, such as Au, Ag, for realizing combined functions of magnetism, optics and biocompatibility. Xu *et al.* reported the synthesis of Au- and Ag-coated Fe_3O_4 NCs with controlled plasmonic and magnetic properties.[158] In the chloroform solution of OAm, Au could be coated on the surface of Fe_3O_4 seeds by reducing $HAuCl_4$. Ag shell could be further generated onto Fe_3O_4/Au NCs by adding $AgNO_3$ to the reaction mixture after the seeds were transferred into water. In order to obtain uniform Au (or Ag) shell, it is essential to enhance the surface energy of Fe_3O_4 to effectively adsorb Au atoms. Among a variety of strategies, surface modifications of Fe_3O_4 by those molecules containing the groups which exhibit strong affinity to Au have been regarded as the most efficient approach. Jin *et al.* found that in contrast to commonly used primary amines, the imidazole groups are capable of immobilizing Au^{3+} ions on Fe_3O_4 at high packing density. The authors used ploy-L-histidine to modify the outer surface of Fe_3O_4, inducing the uniform Au shell growth by the reduction of Au^{3+}.[31]

Core/shell HNCs incorporating magnetic and semiconducting chalcogenides components are worth mentioning. FePt/CdS were produced by series of reactions in a one-pot procedure, whereby FePt NCs were first formed in the solution and were subsequently allowed to react with sulfur and $Cd(acac)_2$ to generate amorphous CdS shell. Notably, the metastable core/shell structure could be transformed into heterodimers of crystalline CdS and FePt NCs upon heating for eliminating the surface tension between the two components.[159] When using FePt NCs as seeds, they could also prepare FePt/CdX (X = S, Se) core/shell NCs by the sequent addition of $Cd(acac)_2$ and chalcogens, whereby FePt/CdO core/shell intermediates were formed for the successful preparation of the final structure.[160] Monodisperse spherical or cube-shaped FePt/PbX (X = S, Se) were generated via similar strategy.[161]

Magnetic materials enwrapped within a biocompatible and hydrophilic SiO_2 shell have attracted increasing interest. The silica shell is beneficial to promote the biocompatibility of the magnetic NCs, such as Fe_3O_4, for the improvement in biochemical applications. The silica shell can also contribute to minimize release of toxic metals to biological environments. In addition, further modification of the silica shell may bring more functions of the system. The main synthetic method to fabricate silica-coated magnetic NCs relies on the reaction in water-in-oil microemulsions. Numerous reports showed that the silica coating could be successfully achieved by microemulsions as nanoreactors, which can efficiently dissolve the precursors and seeds, and control the hydrolysis and condensation reactions. The surfactant, which determines the size of the droplets and in turn strongly affect the coating process, is found to be the key factor to achieve silica-coated magnetic NCs with diverse sizes, shapes, and functions. Though this methodology, FePt/SiO_2, $CoFe_2O_4/SiO_2$, and other ferrites/SiO_2 core/shell NCs could be prepared.[162–167] For example, with the assistance of the surfactant, Igepal CO-520 (poly(5)ox-yethylene-4-nonylphenyl-ether), the FePt NCs were coated with SiO_2 by base-catalyzed silica formation from tetraethyl-orthosilicate in a water-in-oil microemulsion. The silica shell could effectively prevent FePt coalescence even at a high temperature up to 850 °C.[164]

Another commonly used strategy to generate shell on the magnetic core is redox transmetalation reactions between the reagents without the need for any additional reductants. In terms of metal/oxide systems, the metal core, which is usually chemically active toward oxygen, can be easily oxidized to form metal/oxide core/shell nanostructures with controlled shell thickness. Fe/Fe_3O_4,[79] Co/CoO,[168] and Ni/NiO[169] core/shell NCs can be obtained by air exposure or addictive oxidation of the metal seeds. For example, by exposing OAm-capped Fe NCs to air, amorphous iron shell can be introduced (Fig. 8(a)).[79] A crystalline Fe_3O_4 shell could be produced by controlled oxidation of the as-synthesized NCs using an oxygen transferring agent $(CH_3)_3NO$, which effectively made Fe/Fe_3O_4 core/shell NCs more stable (Fig. 8(b)). Through the sacrificial conversion, the magnetic metal cores (Fe or Co) were able to be coated with those metals which are chemically less active and possess favorable redox potentials (such as Au, Pt, Pd). Lee *et al.* reported a general protocol for the synthesis of high-quality Co/M (M = Au, Pd, Pt, Cu) core/shell NCs by redox-transmetalation process in the presence of Co NCs. During the process, the metal ions can be reduced on the surface of Co NCs, while the Co atoms were in turn released as Co-ligand complex. The simultaneous core metal consumption and shell layer formation contribute to the uniformity of the final products (Fig. 8(c)).[170]

Interestingly, the generation of the AFM shell on the FM core offers a good platform to study the exchange bias effects. Sun *et al.* prepared FeO/Fe_3O_4 core/shell NCs with tunable FeO core size and Fe_3O_4 shell thickness via a controlled oxidation process (Fig. 8(d)).[156] Alternatively, MnO/Mn_3O_4[171] and even more complex core/shell nanostructures[149] (three-, and four-component multilayers) can be achieved through similar strategy.

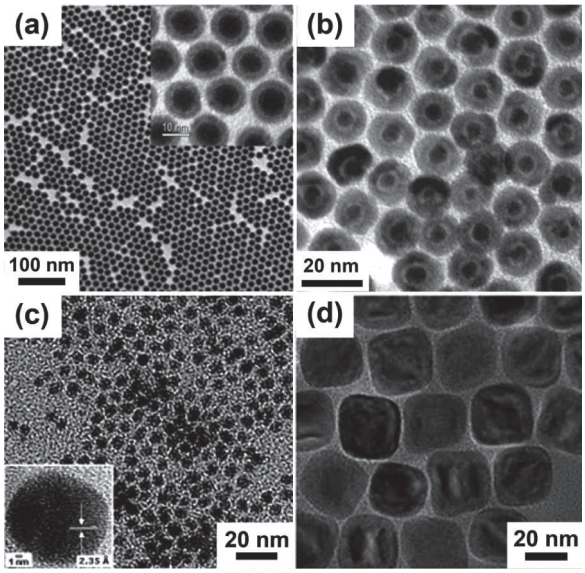


Fig. 8. TEM images of typical core/shell HNCs prepared based on redox transmetalation reactions. (a) and (b) Fe/Fe_3O_4 core/shell HNCs. Reproduced with permission from Ref. [79]. Copyright 2006 American Chemical Society. (c) Co/Au core/shell HNCs. Reproduced with permission from Ref. [170]. Copyright 2005 American Chemical Society. (d) FeO/Fe_3O_4 core/shell HNCs. Reproduced with permission from Ref. [156]. Copyright 2012 American Chemical Society.

Unlike the classical seed-mediated approach, which frequently requires multiple steps to separate the nucleation and growth processes artificially, there have also been successful efforts to develop simplified one-pot single-step methods. In the reaction process, all necessary precursors, which are present simultaneously in the solution, can successively decompose to realize the self-controlled nucleation and growth. Under appropriate conditions, different materials form at distinct times or temperatures, and the shell can be produced by heterogeneous nucleation on the *in-situ* formed seeds. Based on the self-controlled nucleation/growth mechanism, Ag/Co,[172] Cu/Ni,[173] Au/Co,[174] and Cr/Fe_2O_3[175] core/shell NCs can be successfully synthesized. For example, in the one-pot preparation of Au/Co core/shell NCs, Au^{3+} could be first reduced to form Au NCs at low temperature. Afterwards, when the temperature was further increased to 200 °C, the preformed Au seeds were able to catalyze Co nucleation to ensure the continuous shell growth.[174]

3.2. Oligomer-like heterostructure

Apart from core/shell NCs, oligomer-like HNCs are also a distinguished family of heterostructured nanomaterials which incorporate distinct domains of materials interconnected through limited small bonding interfaces. To obtain such oligomer-like topologies, the thermodynamically controlled growth is anisotropically centered on one or several sites of the seeds, which is distinct from the case in the preparation of core/shell HNCs. Therefore, by varying the objective materials and/or tuning the synthetic conditions that can promote anisotropic growth, the oligomer-like geometries can be successfully achieved. For example, materials that hardly form alloys and/or are strongly lattice-uncorrelated tend to form oligomers in order to minimize the interfacial energy. In addition, the environmental parameters, such as the seed-to-precursor ratio, the solution concentration, the heating profile, and the polarity of the solvent play important roles in developing the oligomers. By tuning the concentration of the precursors below the homogeneous nucleation threshold, heterogeneous nucleation is promoted while homogeneous nucleation is suppressed so that the secondary growth preferentially occurs at accessible sites of the seeds. The heating profile can induce the phase segregation, leading to the formation of oligomer-like heterostructures from core/shell geometries by a surface de-wetting process. The polarity of the solvent can strongly affect the electron distribution on the surface of the seeds and electron transfer at the interface, thus one can conveniently obtain the oligomer-like morphologies rather than core/shell nanostructures.

Like core/shell nanostructures, oligomers incorporating magnetic components have received intensive studies. The exchange coupling between the different magnetic domains at the interfaces that are distinct from those of the core/shell NCs, also brings various interesting magnetic phenomenon. Moreover, due to the surface exposure of each component given by the oligomer-like geometries, one can exploit their surface activity to link functional molecules or to make effective catalysis. The magnetic component can not only contribute to magnetically recovery of the catalysts, but also benefit catalytic properties via electron transfer at the interfaces. Such advantages make the magnetic oligomers promising especially in the field of medical diagnosis/therapy and recyclable catalysis.[29,145,176]

The seed-mediated protocols have been successfully utilized in the preparation of various types of magnetic oligomers. In the presence of preformed NCs, Fe_3O_4-X_1 (X_1 = Au, Pt, Ag, Ni, FePt, AuAg),[176–182] CoO/MnO-X_2 (X_2 = Au, Ag, Pt, FePt),[148,179,180,183] and FePt-X_3 (X_3 = $CoFe_2O_4$, Au, CdS, PbS, PbSe)[147,161,184,185] oligomers can be produced by thermal decomposition of the precursors for growth. For example, to prepare Au–Fe_3O_4 dumbbells, Au NCs with different sizes were first synthesized by the reduction of $HAuCl_4$ in OAm.[176,180] In the growth procedure, iron pentacarbonyl, $Fe(CO)_5$, was used as the iron source to intro-

duce the iron growth over the surface of the Au seeds. The joint iron component was transformed to Fe_3O_4 by the following oxidation process. The size of the Fe_3O_4 sections could be tuned by adjusting the $Fe(CO)_5$/Au ratio (Fig. 9). This synthetic approach can be further improved for the preparation of a range Au–Fe_3O_4 hybrid NCs owing more interconnected interfaces with controlled sizes and the numbers of Fe_3O_4 domains by choosing multiply twinned Au NCs as seeds.[181] Generally, the generation of phase segregation by anisotropic growth can be ascribed to the appreciable difference in lattice parameters of connected materials, which strongly affect the interfacial energy. However, in some cases, the polarity of the solvent is found to determine the number of nucleation sites for growth on the seeds. For instance, when Fe_3O_4 is initially nucleated on the Au seeds, electrons will transfer from Au to Fe_3O_4 through the interface, leading to electron deficiency on the Au NCs.[176,177] As long as the electron deficiency is replenished from the electron–donor solvent, multiple nucleation sites can be generated so that flower-like and even core/shell heterostructures can be formed. In contrast, further nucleation events are inhibited caused by the electron deficiency if non-polar solvent is used. Therefore, by modulating the polarity of the solvent, magnetic heterostructures with different topologies can be easily controlled, leading to the potential possibilities for the applications with designed functionalities. In some cases, the morphology of the seeds and the bonding ligand on certain facets were found to be critical to the formation of final heterostructures.[147,161,178] If the cubic FePt NCs are chosen as seeds instead of spherical ones, brick-like FePt/$CoFe_2O_4$ can be prepared.[147] In terms of the synthesis of dumbbell-like FePt–PbS nanostructures, extensive washing of FePt seeds is required to recap OAm ligands with less labile oleate ligands.[161] By tuning the reaction temperature, dumbbell-like structures with size-controlled near-spherical and cubic PbS components attached to FePt NCs can be prepared. Notably, core/shell heterostructures appear if the surface of FePt seeds is extensively treated with an excess of OAm due to more nucleation sites generated by labile amine surfactants. More interestingly, the seed-mediated approach has shown extraordinary effects on achieving more complex heterostructures containing multiple domains by stepwise construction of supplied seeds. This is conceptually analogous to the construction of complex organic molecules, and can be comprehensively understood from a representative example to synthesize M–Pt–Fe_3O_4 (M = Au, Ag, Ni, Pd) heterotrimers, and M_xS–Au–Pt–Fe_3O_4 (M = Pb, Cu) heterotetramers.[186]

Alternatively, oligomers can be formed from metastable core/shell HNCs by thermally driven coalescence/crystallization process. There have been systematic investigations of the formation of oligomer-like heterostructures based on magnetic (FePt, γ-Fe_2O_3) and semiconducting chalcogenides (CdS, ZnS, HgS, CdSe, ZnSe, HgSe),[163,184,186–190] revealing the way of topological change governed by the interfacial strain energy. For example, in the γ-Fe_2O_3–CdS system, a highly defective and amorphous layer of CdS was initially deposited onto the γ-Fe_2O_3 seeds by the sequential addition of sulfur and Cd reagent.[188,189] In spite of the appearance of partial aggregations, the core/shell heterostructures maintained at low temperature would transfer into heterojunctions upon heating the solution at elevated temperature. The significant change can be explained by the large lattice mismatch between γ-Fe_2O_3 and CdS components after CdS gradually became crystalline. By examining the morphology of the products incorporating other surfides (ZnS, HgS) under similar synthetic conditions, the effects of lattice mismatch at the heterojunctions can be obviously addressed. The yield of heterostructures was found to be lower in the systems with larger mismatch, and even complete particle separation could be observed in the HgS system with the largest mismatch.[189] The topologies of the heterojunctiions can be further tuned by varying the seed size and/or the growth rate. In the Fe_3O_4–CdS system, the size of Fe_3O_4 seeds has a strong influence on the interfacial strain, leading to the formation of CdS with different sizes and numbers.[190] When the size of Fe_3O_4 seeds is small, the strain can be relieved so that CdS NCs were able to grow into relatively large sizes, while for seeds larger than 7 nm, the growth of CdS was inhibited and the addition of excess Cd/S reagents would lead to the formation of multiple heterojunctions. Interestingly, rods-on-dot structures could be produced by carefully separating the stages of junction formation and growth, and controlling the growing rates of CdS.

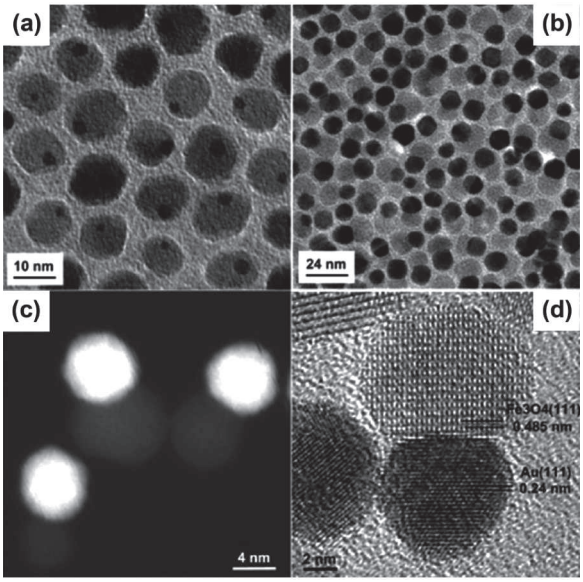


Fig. 9. TEM images of the dumbbell-like Au–Fe_3O_4 HNCs with the size of (a) 3 nm–14 nm and (b) 8 nm–14 nm. (c) HAADF–STEM image of the 8 nm–9 nm Au–Fe_3O_4 HNCs. (d) HRTEM image of one 8 nm–12 nm Au–Fe_3O_4 NC. Reproduced with permission from Ref. [176]. Copyright 2005 American Chemical Society.

Another attractive approach to get magnetic heterojunctions is based on reactions at liquid/liquid interfaces (Fig. 10).[191] In this simple methodology, the organic phase containing NCs (FePt, Fe_3O_4 dissolved in dichlorobenzene, dichloromethane, hexane, or dioctyl ether) is mixed with the aqueous phase containing Ag^+ to form the microemulsion, i.e. "colloidosomes" in aqueous phase, by ultra-sonification. The micro-emulsion can be stabilized by the NCs that self-assemble at a liquid–liquid interface. Since a few Fe(II) sites on the exposed surface of the NCs act as the catalytic center for the reduction of Ag^+, Ag nucleate and grow continuously to form heterodimers as the reduction proceeds. The formation of the heterodimers, rather than core/shell structures, can be ascribed to the fact that the seeds are only partially exposed to the aqueous phase so that metal deposition is restricted to a small surface region. The general synthetic method offers access to FePt–Ag, Fe_3O_4–Ag, hollow γ-Fe_2O_3–Ag heterodimers, which can be applied for protein binding, molecular imaging, and pathogen detections.

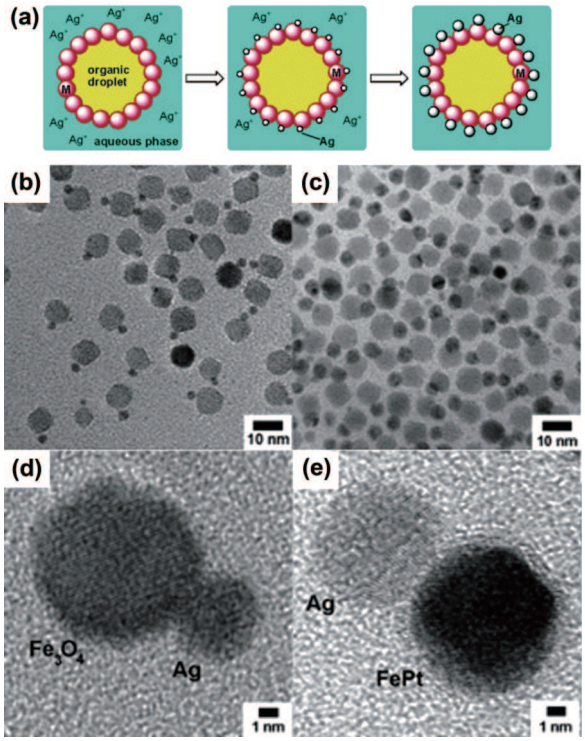


Fig. 10. (a) Schematic illustration of the synthesis of Ag–FePt (Fe_3O_4) heterodimers based on reactions at liquid/liquid interfaces. TEM images of (b) 8 nm–3 nm and (c) 8 nm–5.5 nm Fe_3O_4–Ag heterodimers. HRTEM images of (d) Fe_3O_4–Ag and (e) FePt–Ag heterodimers. Reproduced with permission from Ref. [191]. Copyright 2005 American Chemical Society.

Simplified one-pot method, in which all the reagents are added into the primary solution at the beginning of the synthesis, has also been developed to synthesize magnetic heterostructures. Compared to the classical seed-mediated approach, this method, which is based on self-regulated nucleation/growth, has obvious advantages in avoiding complicated procedures comprised of the preparation of seeds, and the subsequent growth. Nevertheless, identification of the experimental conditions, as well as understanding toward the inherent reaction mechanism are still insufficient and challenging. Such a method has been implemented to synthesize FePt–Fe_3O_4, Au–Ni, and Co–Pd sulfide heterostructures.[174,192,193] Notably, the report of a comprehensive study to prepare FePt–Fe_3O_4 heterodimers via one-pot colloidal approach has represented an advance in this respect.[193] By temperature-driven sequential reactions in an OAm/OA/1-octadecene environment, which involved the homogeneous nucleation of FePt seeds and the subsequent heterogeneous growth of iron oxide, size-controlled synthesis of the heterodimers can be realized. The FePt NCs were first form at low temperature, after which Fe complexes in the solution sustained nucleation and growth of iron oxide on preformed FePt NCs upon thermal decomposition at elevated temperature. The size of the starting FePt NCs and the $Fe(CO)_5$/$Pt(acac)_2$ molar ratio used in the synthesis were found to be critical for the domain dimensions of the heterostructures because they determined the ultimate surface area available for heterogeneous deposition and the growth degree of the iron oxide domain, respectively. Similarly, Au–Ni heterodimers can be obtained by temperature-driven sequential reactions, in which preformed Au NCs could induce the deposition of Ni.[174]

There are also a few attempts to prepare oligomer-like heterostructures, especially those high-order hetero-oligomers, which are made by coupling reactions of smaller fragments to form larger oligomers by certain additives. A typical example can be illustrated for the synthesis of Fe_3O_4–Au–Fe_3O_4 dumbbells, in which Au–Fe_3O_4 heterodimers can be fused together in the presence of sulfur to form ternary dumbbells.[177] Owing to the high affinity to Au, sulfur can be enriched on Au surfaces, and therefore help triggering welding of the Au domains in Au–Fe_3O_4 heterodimers. Inspired by such a unique process, Schaak *et al.* reported the observation of higher-order $(Au–Pt–Fe_3O_4)_n$ hetero-oligomers with distinct geometries (linear, bent, and branched nanostructures) by heating Au–Pt–Fe_3O_4 heterotrimers to 120 °C–150 °C with a trace amount of sulfur powder in trioctylamine.[186]

3.3. Anisotropically shaped material-based heterostructure

Another family of heterostructured magnetic nanomaterials based on anisotropically shaped components is worth mentioning. Heterogeneous growth on anisotropically shaped seeds, such as nanorods, nanowires, and branched NCs, can result in the formation of heterostructures with spatially asymmetric configuration. Notably, the facet-dependent reactivity of the seeds for secondary growth becomes rather pronounced to drive the ways of heterogeneous nucleation compared to

the cases in the formation of core/shell and oligomer-like heterostructures. Based on the minimizing of the overall surface and interfacial energy of the system, nucleation can occur on apexes and sidewalls of the seeds selectively or nonselectively to form distinct architectures. By varying the synthetic conditions, such as solution supersaturation, reactant diffusion, and reaction atmospheres, spherical, linear, and branched growth can be achieved. Due to the coupling and electron transport across the interface between the different domains, this family of heterostructured nanomaterials can exhibit novel or enhanced physical and chemical properties. So far, there has been considerable progress on preparation of semiconductor-based heterostructures relied on the advance in getting their anisotropic shapes. In terms of magnetic heterostructures, there have also been successful efforts to devise pathways to achieve various architectures with designed functionalities.

Based on the controlled growth of Au NCs onto FePt nanorods, tadpole-, dumbbell-, bead-, and necklace-like FePt–Au nanostructures were synthesized.[194] The heterostructures can be tuned by manipulating the reaction atmosphere and the crystallization of FePt seeds. Under an Ar atmosphere, tadpole-like FePt–Au nanostructures were formed from the FePt seeds treated at 300 °C, while dumbbell- and bead-like heterostructures could be obtained by bubbling forming gas into the solution for different time. Since hydrogen possesses the tendency to be adsorbed onto the surface of FePt to freshen their surfaces and lower the reduction energy of Au, the introduction of H_2 can help create more active sites for Au nucleation, otherwise the nucleation preferentially occur on the tips. To further increase the nucleation sites, FePt that synthesized at low temperature (180 °C–220 °C) were used as seeds, from which necklace-like nanostructures were produced under Ar/H_2 atmosphere.

The heterostructures incorporating semiconductor and magnetic all-oxide components, which can be envisioned to enable exploitation of multifunctional nanomaterials, have attracted much attention. In the synthesis of TiO_2–Fe_xO_y heterostructures, the rod-like TiO_2 seeds with size- and shape-dependent anisotropic reactivity were found to strongly affect the selective heterogeneous nucleation and growth of iron oxide, leading to various final architectures.[195–197] Iron oxide with controlled sizes and numbers could be kinetically overdriven toward active regions of the exposed b-TiO_2 facets by multi-step hot-injection of $Fe(CO)_5$/OA/1-octadecene. Compared to anatase TiO_2, brookite seeds with enhanced reactivity were found to be capable to overcome strain-related heteroepitaxial growth constraints.[197] Additionally, for larger TiO_2 seeds, multiple deposition of iron oxide were encouraged so that architectures with more iron oxide domains could be obtained. Further investigations by the same group[196] indicated that under diffusion-controlled growth conditions, iron oxide can be epitaxially grown at either one apex or any location along their longitudinal sidewalls of b-TiO_2 nanorods distinguished by a curved shape-tapered profile with richly faceted terminations (Fig. 11). By taking advantage of the generation of strain fields during heteroepitaxial growth, heterostructures of iron oxide decorated on the longitudinal facets of TiO_2 nanorods have been prepared. It was revealed that the strain played an important role in the formation of the architectures due to the fact that the two domains of TiO_2 and iron oxide share a restricted and locally curved junction region, which efficiently accommodates the interfacial strain and retards the formation of misfit dislocations.

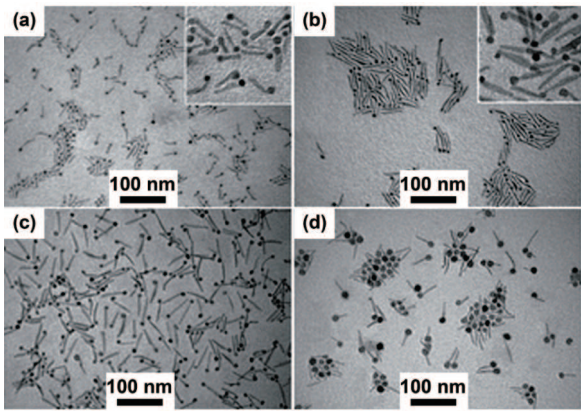


Fig. 11. (a)–(d) TEM images of matchstick-shaped HNCs based on b-TiO_2 nanorod seeds with different sizes and aspect ratios. Reproduced with permission from Ref. [196]. Copyright 2010 American Chemical Society.

Alternatively, there have been some reports on the syntheses of magnetic-metal/semiconductor heterostructures based on the domains with anisotropic shape prepared by colloidal methods. In the heterostructures of CdS (CdSe) nanorods decorated with magnetic metals (PtCo, Co), metal nucleation can be successfully realized at both seed apexes in a high degree of selectivity.[198–201] For example, CdSe/Co nanorod/nanosphere hybrid NCs could be obtained through the selective growth of cobalt on the tips of CdSe nanorods, while the formation CdSe/Co nanorod/nanorod heterostructure could be observed at elevated reaction temperature by inducing anisotropic growth of the initially formed Co nanospheres.[198] However, in the presence of nanowires, the metal deposition occurs nonselective, leading to multiple metal domains on apex and any location along the longitudinal sidewalls of the nanowires.[199]

In the previous parts, surfactants or ligands that facet-preferentially adhere onto the surfaces of the seeds have been revealed to be critical for preparing core/shell and oligomer-like heterostructures. Similarly, by exploiting anisotropic nanomaterials as seeds, the selective heterogeneous nucleation is also strongly dependent on the molecule attachment of the seeds. In many cases, surfactant concentration is kept at a

relatively low value to ensure sufficient heterogeneous nucleation. Due to the large lattice mismatch, the effects of surfactants have been found to be pronounced to incorporate oxide and metal. Size-tailored ZnO nanorods decorated with magnetic Fe-based domains, were synthesized via a colloidal seeded-growth method in a noncoordinating solvent.[202] In surfactant-free 1-octadecene, a variable number of Fe/Fe_xO_y core/shell NCs with no facet-preferential attachment could be grown onto purified ZnO nanorods by the controlled hot-injection of $Fe(CO)_5$, followed by air-oxidation. The surfactant-free environment was also exploited to grow Co on CdSe/CdS nanorods and γ-Fe_2O_3 tetrapods by $Co_2(CO)_8$ decomposition.[203,204] In the synthesis of three-component Co/CdSe/CdS nanohybrid, metallic Co could be attached to either apexes of one rod-shaped section due to the peculiar anisotropic reactivity of the noncentrosymmetric CdSe/CdS core/shell nanorods.[203] When γ-Fe_2O_3 tetrapods were used as seeds, heterogeneous nucleation, and growth of multiple secondary Co components can be selectively accomplished, leading to tetrapod-shaped skeleton of iron oxide functionalized with multiple domains of Co.[204] The heterostructurers incorporating FiM and FM components exhibit various unique magnetic properties based on the exchange coupling effects between different domains. Notably, in both cases discussed above, the delayed addition of OA could not only restrict Co growth but also promote the colloidal stability of the obtained heterostructures. Co-decorated TiO_2 nanorods were synthesized by thermal decomposition of $Co_2(CO)_8$ under assistance of octanoic acid and OAm, in which heterogeneous Co nucleation in a tip-preferential or a nonselective way could be altered by varying the octanoic acid/OAm concentration.[205] It was suggested that the decrease of surfactant concentration was key to enhance the reactivity of TiO_2, thus TiO_2 seeds were chemically accessible for heterogeneous nucleation. Subsequent addition of OA, which possesses strong affinity to both TiO_2 and Co surfaces, would quench any further reaction owing to the compact organic shell built by bulky OA around the heterostructures.

4. Chemical synthesis of hollow/porous magnetic NCs

Over past decades, researchers have focused on hollow/porous magnetic NCs due to their unique structures and related wide applications.[36,38–41,206] Owing to the hollow interior, porous shell and much higher surface to volume ratio compared to the solid counterparts, hollow/porous magnetic NCs exhibit great potentials in catalysis, water purification, and drug delivery. The interior void can serve as a container for encapsulating active and functional materials, such as NCs, drugs, and proteins, which can be sealed for protection or be made accessible to the outside in many biomedical applications. On the other hand, the porous shell can provide active surfaces for attracting molecules and can offer channels for materials transportation. To synthesize various hollow/porous magnetic NCs, several colloidal synthetic methods have been developed, including the Kirkendall effect, chemical etching, galvanic replacement, and template-mediated approach. In this part, we briefly review recent advance in the synthesis of hollow/porous magnetic NCs, including Fe-based and Mn-based NCs.

4.1. Fe-based hollow/porous NCs

As one of the most popular Fe-based NCs, iron oxide NCs have been intensively investigated for many years due to their relatively high chemical stability and feasibility to obtain. Hollow/porous iron oxide NCs of Fe_3O_4 and Fe_2O_3 with controlled cavity dimension, shell thickness, and porosity have been developed recently. Among those synthetic strategies, the template-assisted approach is regarded as the most convenient and versatile procedure for the synthesis of hollow nanostructures. To synthesize the hollow nanocapsules of iron oxide with porous shells, a wrap-bake-peel process involving SiO_2-templated growth was applied.[42] The spindle-shaped akagenite (β-FeOOH) nanorods were coated with silica, followed by a heat treatment and silica removal. Since significant volume change occurred when a loose akagenite structure changed to a dense haematite phase, iron oxide was able to become hollow/porous structure. Similarly, the magnetite Fe_3O_4 nanocapsules could also be obtained by a simple additional treatment of the heamatite/silica nanocomposite at 500 °C under H_2 atmosphere. The prepared heamatite and magnetite nanocapsules showed typical characteristics of paramagnetism and supermagnetism, respectively. By using carbon NCs as the template, hollow heamatite NCs could also be synthesized via sonochemical method.[207] As the starting materials, Fe/carbon nanocomposites would transferred into hollow α-Fe_2O_3 NCs upon exposure to air. In the procedure, iron shell on the carbon NCs was oxidized while auto-ignition of carbon conducted at the same time, leaving the final hollow oxide nanostructures. Organic micelles have been also utilized as the template to prepare akagenite (β-FeOOH) nanotubes.[208] The uniform hollow nanostructures were achieved when reacting-hydrazine with Fe–oleate complex in reverse micelles formed by OA, xylene, and water. Alternatively, the Kirkendall effect can also be utilized to create hollow/porous nanostructures. In 2004, Alivisatos and his co-workers reported the preparation of hollow CoS (CoO) by sulfidation (oxidation) of Co NCs exploiting the Kirkendall effect at the nanometer scale.[206] During the reaction, the outward element diffusion was faster than the inward diffusion, and consequently the void at the center formed. By similar strategy, monodisperse hollow Fe_3O_4

NCs can be obtained via solution phase synthesis.[209] The amorphous Fe/Fe_3O_4 core/shell NCs were made by thermal decomposition of iron pentacarbonyl, $Fe(CO)_5$ in the presence of OAm and subsequent air oxidation. The controlled oxidation was realized in the presence of oxygen transfer reagent, trimethylamine-N-oxide, Me_3NO. It was observed that in the middle of the reaction process multiple voids were formed in the particle. During the reaction, the solid NCs were transformed into the core/shell/void, the yolk/shell, and, finally, the hollow structures, which was dominated by the Kirkendall effect. It was revealed that the initial Fe/Fe_3O_4 core/shell NCs were essential to create unbalanced interfacial diffusion between oxygen and Fe atoms during the oxidation process, thus resulting in final hollow structures. When the obtained hollow NCs were treated at high temperature, the Fe_3O_4 domain in the shell grew into larger crystallites, leading to the change of the crystal boundaries and formation of the porous shell (Fig. 12).[210] Since the boundary area was more reactive to be etched away, the pore size could be further controlled readily by acid etching. Through similar controlled oxidation process, colloidal solutions of monodisperse iron/iron oxide core–void–shell nanostructures and hollow maghemite NCs with controllable particle size and shell thickness could be produced under an oxygen atmosphere.[211] Etching is also regarded as one effective approach to prepare hollow/porous nanocrtystals. The Hyeon group reported a reproducible and general etching method to synthesize series of hollow oxide NCs with various sizes, shapes, and compositions.[212] The hollow iron oxide of Fe_3O_4 and α-Fe_2O_3 NCs could be obtained by simply heating initial solid NCs in technical grade TOPO at 300 °C for hours. The control experiments revealed that alkylphosphonic acid impurity in TOPO contributed to the diffusion of phosphorus and ironcations in the etching process, which dominated the formation of hollow structures.

Besides the hollow/porous iron oxide NCs, other kinds of Fe-based hollow/porous NCs were also reported. The Hyeon group reported the synthesis of hollow iron nanoframe from the thermal decomposition of the Fe(II)–stearate complex in the presence of sodium oleate and OA.[213] The thermal decomposition of iron salts in the organic solution was generally utilized to synthesize dispersible iron oxide NCs with controlled size, shape, and composition. However, in their process, it was believed that the sodium oleate played an important role in the formation of iron nanoframe due to the fact that sodium molten salt derived from sodium oleate could cause severe corrosion of metallic materials at high temperature. Star-shaped iron nanoframes could also be obtained by decreasing the heating rate. When exposed to air, those iron nanoframes with different structures can be readily transferred to iron oxide nanoframes. Zhao *et al.* successfully achieved monodisperse iron phosphate nanospheres with nanoporous structure through a solvent extraction route using an acid-base-coupled extractant.[214] The established reverse micelles with micro water-pools inside acted as nanoreactors, which can prevent the particles from aggregation. The novel nanoporous structure of the iron phosphate nanospheres is ascribed to the subsequent extractant removal from the nanospheres by organic solvents like acetone or ethanol.

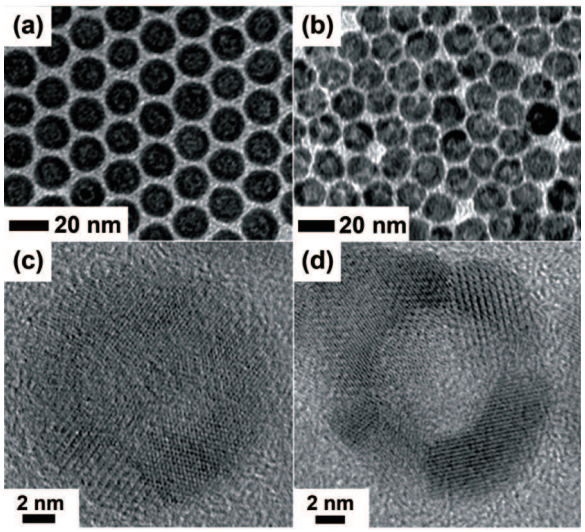


Fig. 12. (a) TEM and (c) HRTEM images of the 16-nm Fe_3O_4 hollow NCs. (b) TEM and (d) HRTEM images of the 16-nm Fe_3O_4 hollow/porous NCs. Reproduced with permission from Ref. [210]. Copyright 2009 American Chemical Society.

4.2. Mn-based hollow/porous NCs

Hollow/porous Mn-based NCs also have important applications in the field of medical diagnosis and therapy. The approach based on etching or Kirkendall effect to hollow/porous Fe-based NCs can be extended to the synthesis of Mn-based NCs. Based on the etching process, An *et al.* fabricated uniform hollow spherical and dumbbell-shaped MnO NCs in the presence of TOPO and alkylphosphonic acid.[212] It was revealed that the impurities in technical grade TOPO, especially alkylphosphonicacid, played important roles in controlling the etching process dominating the formation of hollow structures. The possible mechanism was suggested to be the opposite diffusion of phosphorus and metal cations within the NCs accompanied by Kirkendall effect. Shin *et al.* developed hollow manganese oxide NCs as multifunctional agents for simultaneous MRI and drug delivery.[215] Manganese oxide NCs with a diameter of 20 nm stabilized by OA were initially prepared, and then were transformed to water by encapsulated with poly(ethylene glycol) phospholipid. Afterwards, phthalate buffer solution at pH 4.6 was used to create the hollow interior of the NCs by selective etching of the core MnO phase from the NCs. By varying the duration of immersion of the solid manganese oxide NCs in water before the acid treatment, the interior shape of the hollow NCs could be changed. Immersion for one day afforded an interior cavity with roughly

spherical shape and a diameter of 12 nm, while immersion for $10 \sim 40$ days yielded two or three irregularly shaped cavities having average diameters of 8 nm–5 nm within a particle. Similarly, Kim *et al.* obtained silica-coated hollow MnO NCs via an etching process in the mild hydrochloric acid solution (4%) (pH≈2.4).[216] Alternatively, Peng *et al.* employed a facile method to prepare hollow manganese oxide NCs, wherein the hollow structure was formed by the extrusion of the core MnO via Kirkendall effect with the aid of carboxylate anion.[217]

Recently, Hao *et al.* demonstrated a general strategy to prepare various kinds of hollow/porous Mn-based NCs via directional ion transfer across different solid–liquid interfaces in a one-pot solvothermal process.[218] In a typical procedure, hollow Mn oxide, hollow Mn phosphate, and porous Mn phosphate could be obtained by the reaction of water, $Mn(acac)_2$, and triethyl phosphate under solvothermal conditions in the presence of OA and OAm. It was found that surfactants (OA and OAm) ratios were essential for the void structure and composition of the hollow/porous NCs, and as a result, hollow Mn oxide NCs were formed without OA, while hollow Mn phosphate and porous Mn phosphate NCs were yielded by increasing the amount of OA. Interestingly, these Mn-based porous/hollow NCs can act as effective multifunctional probes for selective diagnosis with MRI, as well as giving efficient targeted drug delivery.[219]

5. Summary and perspectives

Research into colloidal chemical synthesis of magnetic NCs has made substantial progress over the past decades. The size, shape, and composition of magnetic NCs can be effectively controlled through the judicious selection of precursor, solvent, and capping agent. Additionally, size monodispersity, which is critical for many technologically important applications, can also be successfully realized through solution-phase methods. Among those single-component magnetic NCs, metal oxides, especially iron oxide, have attracted the most attention for their wide application potential. For example, size-, crystallinity-, uniformity-controlled iron oxide NCs can be prepared via colloidal chemical synthesis to meet the requirements of diverse biomedical applications. Owing to the superior biocompatibility, iron oxide NC-based MR contrast agents have already been used in clinical trials, or are undergoing clinical trials. Multi-component magnetic NCs with different levels of complexity have also received many investigations recently. Solution-phase method can be utilized as an efficient tool to construct the architectures for designed functionality and performance by purposefully choosing the seeds, and artificially controlling the secondary growth process. The interactions between the joint domains can also bring various interesting chemical–physical phenomena, resulting in unprecedented properties. Furthermore, chemical synthesis of hollow/porous magnetic NCs is highlighted in this review. Based on strategies including the Kirkendall effect, chemical etching, galvanic replacement, and template-mediated approach, various types of Fe-based and Mn-based ones can be successfully prepared. The fine control of the size, uniformity, void and pore structure, and shell thickness help hollow/porous NCs to be suitable as multimodal nanoprobe/carriers for both drug delivery and bioimaging.

However, synthesis of high-quality magnetic NCs practically still remains a challenge. A large scale synthesis of magnetic NCs via green chemistry process is highly demanded. Additionally, extensive studies are needed to maintain the stability of the NCs for a long time without agglomeration or precipitation. For magnetic NCs that are sensitive to air or water, such as metallic Fe, Co, Ni NCs, it is necessary to develop efficient strategies to improve their chemical stability and make the best of their magnetic properties. Nanosized magnetic metal carbides are promising due to their good air stability with high magnetization. Unfortunately, there is no reliable method to control the phase, size, and uniformity of carbide NCs. In the complex HNCs systems, it yet remains a challenge to synthesize elaborate HNCs incorporating nonhomologous and/or structurally uncorrelated materials, and understand the compositional, structural, and topological evolution of nanoheterostructures in detail. Moreover, in the reported synthesis of hollow/porous magnetic NCs, understanding of the mechanism in the structural formation, as well as the characterization techniques, needs to be improved. In the future, the development of the chemical synthesis of magnetic NCs with controlled size, shape, composition, and topology will deliver exciting opportunities in practical exploitation of various magnetic nanomaterials. We expect that magnetic NCs will keep occupying important positions in biomedical, catalytic, and magnetic fields.

References

[1] Sun S, Murray C B, Weller D, Folks L and Moser A 2000 *Science* **287** 1989

[2] Lu A H, Schmidt W, Matoussevitch N, Bönnemann H, Spliethoff B, Tesche B, Bill E, Kiefer W and Schüth F 2004 *Angew. Chem.* **116** 4403

[3] Tsang S C, Caps V, Paraskevas I, Chadwick D and Thompsett D 2004 *Angew. Chem.* **116** 5763

[4] Mornet S, Vasseur S, Grasset F, Veverka P, Goglio G, Demourgues A, Portier J, Pollert E and Duguet E 2006 *Prog. Solid State Chem.* **34** 237

[5] Modo M, Hoehn M and Bulte J W 2005 *Mol. Imaging* **4** 143

[6] Sonvico F, Dubernet C, Colombo P and Couvreur P 2005 *Curr. Pharm. Design* **11** 2091

[7] Frey N A, Peng S, Cheng K and Sun S 2009 *Chem. Soc. Rev.* **38** 2532

[8] Pankhurst Q A, Connolly J, Jones S K and Dobson J 2003 *J. Phys. D: Appl. Phys.* **36** R167

[9] Jain T K, Morales M A, Sahoo S K, Leslie-Pelecky D L and Labhasetwar V 2005 *Mol. Pharm.* **2** 194

[10] Chourpa I, Douziech-Eyrolles L, Ngaboni-Okassa L, Fouquenet J F, Cohen-Jonathan S, Souce M, Marchais H and Dubois P 2005 *Analyst* **130** 1395

[11] Elliott D W and Zhang W X 2001 *Environ. Sci. Technol.* **35** 4922

[12] Takafuji M, Ide S, Ihara H and Xu Z 2004 *Chem. Mater.* **16** 1977
[13] Jeong U, Teng X, Wang Y, Yang H and Xia Y 2007 *Adv. Mater.* **19** 33
[14] Lu A H, Salabas E L and Schüth F 2007 *Angew. Chem. Int. Ed.* **46** 1222
[15] Yu J, Huang D Y, Yousaf M Z, Hou Y L and Gao S 2013 *Chin. Phys. B* **22** 027506
[16] Ho D, Sun X and Sun S 2011 *Acc. Chem. Res.* **44** 875
[17] Yoo D, Lee J H, Shin T H and Cheon J 2011 *Acc. Chem. Res.* **44** 863
[18] Colombo M, Carregal-Romero S, Casula M F, Gutierrez L, Morales M P, Boehm I B, Heverhagen J T, Prosperi D and Parak W J 2012 *Chem. Soc. Rev.* **41** 4306
[19] Jun Y W, Choi J S and Cheon J 2006 *Angew. Chem. Int. Ed.* **45** 3414
[20] Donega C D 2011 *Chem. Soc. Rev.* **40** 1512
[21] Zheng H, Li Y, Liu H, Yin X and Li Y 2011 *Chem. Soc. Rev.* **40** 4506
[22] Carbone L and Cozzoli P D 2010 *Nano Today* **5** 449
[23] Leung K C F, Xuan S H, Zhu X M, Wang D W, Chak C P, Lee S F, Ho W K W and Chung B C T 2012 *Chem. Soc. Rev.* **41** 1911
[24] Lim J and Majetich S A 2013 *Nano Today* **8** 98
[25] Behrens S 2011 *Nanoscale* **3** 877
[26] Wei S Y, Wang Q, Zhu J H, Sun L Y, Lin H F and Guo Z H 2011 *Nanoscale* **3** 4474
[27] Gao J H, Gu H W and Xu B 2009 *Acc. Chem. Res.* **42** 1097
[28] Zeng H and Sun S 2008 *Adv. Funct. Mater.* **18** 391
[29] Hao R, Xing R J, Xu Z C, Hou Y L, Gao S and Sun S H 2010 *Adv. Mater.* **22** 2729
[30] Bigall N C, Parak W J and Dorfs D 2012 *Nano Today* **7** 282
[31] Jin Y, Jia C, Huang S W, O'Donnell M and Gao X 2010 *Nat. Commun.* **1** 41
[32] Jonker B T, Park Y D, Bennett B R, Cheong H D, Kioseoglou G and Petrou A 2000 *Phys. Rev. B* **62** 8180
[33] Skumryev V, Stoyanov S, Zhang Y, Hadjipanayis G, Givord D and Nogues J 2003 *Nature* **423** 850
[34] Zeng H, Li J, Liu J P, Wang Z L and Sun S 2002 *Nature* **420** 395
[35] Li Y, Zhang Q, Nurmikko A V and Sun S 2005 *Nano Lett.* **5** 1689
[36] Li G L, Mohwald H and Shchukin D G 2013 *Chem. Soc. Rev.* **42** 3628
[37] He Q, Wu Z and Huang C 2012 *J. Nanosci. Nanotechnol.* **12** 2943
[38] An K and Hyeon T 2009 *Nano Today* **4** 359
[39] Cheng K and Sun S 2010 *Nano Today* **5** 183
[40] Zhang Q, Wang W, Goebl J and Yin Y 2009 *Nano Today* **4** 494
[41] Lou X W, Archer L A and Yang Z 2008 *Adv. Mater.* **20** 3987
[42] Piao Y, Kim J, Na H B, Kim D, Baek J S, Ko M K, Lee J H, Shokouhimehr M and Hyeon T 2008 *Nat. Mater.* **7** 242
[43] Liu J, Qiao S Z, Hu Q H and Lu G Q 2011 *Small* **7** 425
[44] Park J, Joo J, Kwon S G, Jang Y and Hyeon T 2007 *Angew. Chem. Int. Ed.* **46** 4630
[45] Kwon S G and Hyeon T 2008 *Acc. Chem. Res.* **41** 1696
[46] Laurent S, Forge D, Port M, Roch A, Robic C, Elst L V and Muller R N 2008 *Chem. Rev.* **108** 2064
[47] Jiang W Q, Yang H C, Yang S Y, Horng H E, Hung J C, Chen Y C and Hong C Y 2004 *J. Magn. Magn. Mater.* **283** 210
[48] Dacoata G M, Degrave E, Debakker P M A and Vandenberghe R E 1994 *J. Solid State Chem.* **113** 405
[49] Deng Y, Wang L, Yang W, Fu S and Elaissari A 2003 *J. Magn. Magn. Mater.* **257** 69
[50] Abu Mukh-Qasem R and Gedanken A 2005 *J. Colloid Interface Sci.* **284** 489
[51] Hyeon T, Lee S S, Park J, Chung Y and Na H B 2001 *J. Am. Chem. Soc.* **123** 12798
[52] Wu M Z, Xiong Y, Jia Y S, Niu H L, Qi H P, Ye J and Chen Q W 2005 *Chem. Phys. Lett.* **401** 374
[53] Zhang Z T, Blom D A, Gai Z, Thompson J R, Shen J and Dai S 2003 *J. Am. Chem. Soc.* **125** 7528
[54] Lee J, Zhang S and Sun S 2013 *Chem. Mater.* **25** 1293
[55] Laurent S, Forge D, Port M, Roch A, Robic C, Vander Elst L and Muller R N 2008 *Chem. Rev.* **108** 2064
[56] Lee N and Hyeon T 2012 *Chem. Soc. Rev.* **41** 2575
[57] Ling D and Hyeon T 2013 *Small* **9** 1450
[58] Kang Y S, Risbud S, Rabolt J F and Stroeve P 1996 *Chem. Mater.* **8** 2209
[59] Fried T, Shemer G and Markovich G 2001 *Adv. Mater.* **13** 1158
[60] Tang Z X, Sorensen C M, Klabunde K J and Hadjipanayis G C 1991 *J. Colloid Interface Sci.* **146** 38
[61] Zhang Z J, Wang Z L, Chakoumakos B C and Yin J S 1998 *J. Am. Chem. Soc.* **120** 1800
[62] Massart R 1981 *IEEE Trans. Magn.* **17** 1247
[63] Sun S, Zeng H, Robinson D B, Raoux S, Rice P M, Wang S X and Li G 2003 *J. Am. Chem. Soc.* **126** 273
[64] Park J, An K, Hwang Y, Park J G, Noh H J, Kim J Y, Park J H, Hwang N M and Hyeon T 2004 *Nat. Mater.* **3** 891
[65] Kim D, Lee N, Park M, Kim B H, An K and Hyeon T 2008 *J. Am. Chem. Soc.* **131** 454
[66] Kim B H, Lee N, Kim H, An K, Park Y I, Choi Y, Shin K, Lee Y, Kwon S G, Na H B, Park J G, Ahn T Y, Kim Y W, Moon W K, Choi S H and Hyeon T 2011 *J. Am. Chem. Soc.* **133** 12624
[67] Hou Y, Xu Z and Sun S 2007 *Angew. Chem.* **119** 6445
[68] Buonsanti R and Milliron D J 2013 *Chem. Mater.* **25** 1305
[69] Lee J H, Huh Y M, Jun Y, Seo J, Jang J, Song H T, Kim S, Cho E J, Yoon H G, Suh J S and Cheon J 2007 *Nat. Med.* **13** 95
[70] Jang J T, Nah H, Lee J H, Moon S H, Kim M G and Cheon J 2009 *Angew. Chem. Int. Ed.* **48** 1234
[71] Noh S H, Na W, Jang J T, Lee J H, Lee E J, Moon S H, Lim Y, Shin J S and Cheon J 2012 *Nano Lett.* **12** 3716
[72] Huber D L 2005 *Small* **1** 482
[73] Arruebo M, Fernandez-Pacheco R, Ibarra M R and Santamaria J 2007 *Nano Today* **2** 22
[74] Wang C B and Zhang W X 1997 *Environ. Sci. Technol.* **31** 2154
[75] Meffre A, Lachaize S, Gatel C, Respaud M and Chaudret B 2011 *J. Mater. Chem.* **21** 13464
[76] Lacroix L M, Lachaize S B, Falqui A, Respaud M and Chaudret B 2008 *J. Am. Chem. Soc.* **131** 549
[77] Dumestre F, Chaudret B, Amiens C, Renaud P and Fejes P 2004 *Science* **303** 821
[78] Lacroix L M, Frey Huls N, Ho D, Sun X, Cheng K and Sun S 2011 *Nano Lett.* **11** 1641
[79] Peng S, Wang C, Xie J and Sun S H 2006 *J. Am. Chem. Soc.* **128** 10676
[80] Lisiecki I, Albouy P A and Pileni M P 2003 *Adv. Mater.* **15** 712
[81] Wang Z L, Dai Z and Sun S 2000 *Adv. Mater.* **12** 1944
[82] Dumestre F, Chaudret B, Amiens C, Fromen M C, Casanove M J, Renaud P and Zurcher P 2002 *Angew. Chem.* **114** 4462
[83] Dinega D P and Bawendi M G 1999 *Angew. Chem. Int. Ed.* **38** 1788
[84] Sun S and Murray C B 1999 *J. Appl. Phys.* **85** 4325
[85] Petit C and Pileni M P 1999 *J. Phys. Chem. B* **103** 1805
[86] Puntes V F, Krishnan K M and Alivisatos A P 2001 *Science* **291** 2115
[87] Puntes V F, Krishnan K M and Alivisatos P 2001 *Appl. Phys. Lett.* **78** 2187
[88] Murray C B, Sun S, Gaschler W, Doyle H, Betley T A and Kagan C R 2001 *IBM J. Res. Dev.* **45** 47
[89] Puntes V F, Zanchet D, Erdonmez C K and Alivisatos A P 2002 *J. Am. Chem. Soc.* **124** 12874
[90] Winnischofer H, Rocha T C R, Nunes W C, Socolovsky L M, Knobel M and Zanchet D 2008 *ACS Nano* **2** 1313
[91] Zhang H T, Wu G, Chen X H and Qiu X G 2006 *Mater. Res. Bull.* **41** 495
[92] Cordente N, Respaud M, Senocq F, Casanove M J, Amiens C and Chaudret B 2001 *Nano Lett.* **1** 565
[93] Chen Y, Peng D L, Lin D and Luo X 2007 *Nanotechnology* **18** 505703
[94] Mourdikoudis S, Simeonidis K, Vilalta-Clemente A, Tuna F, Tsiaoussis I, Angelakeris M, Dendrinou-Samara C and Kalogirou O 2009 *J. Magn. Magn. Mater.* **321** 2723
[95] Sun S 2006 *Adv. Mater.* **18** 393
[96] Wang J P 2008 *Proc. IEEE* **96** 1847
[97] Chen M, Liu J P and Sun S 2004 *J. Am. Chem. Soc.* **126** 8394
[98] Chen M, Kim J, Liu J P, Fan H and Sun S 2006 *J. Am. Chem. Soc.* **128** 7132
[99] Lee J H, Jang J T, Choi J S, Moon S H, Noh S H, Kim J W, Kim J G, Kim I S, Park K I and Cheon J 2011 *Nat. Nanotechnol.* **6** 418
[100] Kim J, Rong C, Liu J P and Sun S 2009 *Adv. Mater.* **21** 906
[101] Kim J, Lee Y and Sun S 2010 *J. Am. Chem. Soc.* **132** 4996
[102] Yamamoto S, Morimoto Y, Tamada Y, Takahashi Y K, Hono K, Ono T and Takano M 2006 *Chem. Mater.* **18** 5385
[103] Rong C B, Li D, Nandwana V, Poudyal N, Ding Y, Wang Z L, Zeng H and Liu J P 2006 *Adv. Mater.* **18** 2984

[104] Jeyadevan B, Urakawa K, Hobo A, Chinnasamy N, Shinoda K, Tohji K, Djayaprawira D D J, Tsunoda M and Takahashi M 2003 *Jpn. J. Appl. Phys.* **242** L350

[105] Howard L E M, Nguyen H L, Giblin S R, Tanner B K, Terry I, Hughes A K and Evans J S O 2005 *J. Am. Chem. Soc.* **127** 10140

[106] Chaubey G S, Barcena C, Poudyal N, Rong C, Gao J, Sun S and Liu J P 2007 *J. Am. Chem. Soc.* **129** 7214

[107] Desvaux C, Amiens C, Fejes P, Renaud P, Respaud M, Lecante P, Snoeck E and Chaudret B 2005 *Nat. Mater.* **4** 750

[108] Wang C, Peng S, Lacroix L M and Sun S 2009 *Nano Res.* **2** 380

[109] de Smit E, Cinquini F, Beale A M, Safonova O V, van Beek W, Sautet P and Weckhuysen B M 2010 *J. Am. Chem. Soc.* **132** 14928

[110] Torres Galvis H M, Bitter J H, Khare C B, Ruitenbeek M, Dugulan A I and de Jong K P 2012 *Science* **335** 835

[111] Giordano C, Kraupner A, Wimbush S C and Antonietti M 2010 *Small* **6** 1859

[112] Kim J H, Kim J, Park J H, Kim C K, Yoon C S and Shon Y 2007 *Nanotechnology* **18** 115609

[113] Herrmann I K, Grass R N, Mazunin D and Stark W J 2009 *Chem. Mater.* **21** 3275

[114] Yang C, Zhao H, Hou Y and Ma D 2012 *J. Am. Chem. Soc.* **134** 15814

[115] Meffre A, Mehdaoui B, Kelsen V, Fazzini P F, Carrey J, Lachaize S, Respaud M and Chaudret B 2012 *Nano Lett.* **12** 4722

[116] Harris V G, Chen Y, Yang A, Yoon S, Chen Z, Geiler A L, Gao J, Chinnasamy C N, Lewis L H, Vittoria C, Carpenter E E, Carroll K J, Goswami R, Willard M A, Kurihara L, Gjoka M and Kalogirou O 2010 *J. Phys. D: Appl. Phys.* **43** 165003

[117] Huba Z J and Carpenter E E 2012 *J. Appl. Phys.* **111** 07B529

[118] Zhang Y, Chaubey G S, Rong C, Ding Y, Poudyal N, Tsai P C, Zhang Q and Liu J P 2011 *J. Magn. Magn. Mater.* **323** 1495

[119] An K, Lee N, Park J, Kim S C, Hwang Y, Park J G, Kim J Y, Park J H, Han M J, Yu J and Hyeon T 2006 *J. Am. Chem. Soc.* **128** 9753

[120] Goto Y, Taniguchi K, Omata T, Otsuka-Yao-Matsuo S, Ohashi N, Ueda S, Yoshikawa H, Yamashita Y, Oohashi H and Kobayashi K 2008 *Chem. Mater.* **20** 4156

[121] Schaefer Z L, Weeber K M, Misra R, Schiffer P and Schaak R E 2011 *Chem. Mater.* **23** 2475

[122] Prins R and Bussell M E 2012 *Catal. Lett.* **142** 1413

[123] Brock S L and Senevirathne K 2008 *J. Solid State Chem.* **181** 1552

[124] Muthuswamy E, Kharel P R, Lawes G and Brock S L 2009 *ACS Nano* **3** 2383

[125] Muthuswamy E, Savithra G H L and Brock S L 2011 *ACS Nano* **5** 2402

[126] Senevirathne K, Burns A W, Bussell M E and Brock S L 2007 *Adv. Funct. Mater.* **17** 3933

[127] Brock S L, Perera S C and Stamm K L 2004 *Chem. Eur. J.* **10** 3364

[128] Henkes A E and Schaak R E 2007 *Chem. Mater.* **19** 4234

[129] Zheng X F, Yuan S L, Tian Z M, Yin S Y, He J H, Liu K L and Liu L 2009 *Chem. Mater.* **21** 4839

[130] Ha D H, Moreau L M, Bealing C R, Zhang H T, Hennig R G and Robinson R D 2011 *J. Mater. Chem.* **21** 11498

[131] Lo C T and Kuo P Y 2010 *J. Phys. Chem. C* **114** 4808

[132] Henkes A E, Vasquez Y and Schaak R E 2007 *J. Am. Chem. Soc.* **129** 1896

[133] Park J, Koo B, Yoon K Y, Hwang Y, Kang M, Park J G and Hyeon T 2005 *J. Am. Chem. Soc.* **127** 8433

[134] Qian C, Kim F, Ma L, Tsui F, Yang P and Liu J 2004 *J. Am. Chem. Soc.* **126** 1195

[135] Zhang H T, Ha D H, Hovden R, Kourkoutis L F and Robinson R D 2011 *Nano Lett.* **11** 188

[136] Perera S C, Fodor P S, Tsoi G M, Wenger L E and Brock S L 2003 *Chem. Mater.* **15** 4034

[137] Park J, Koo B, Hwang Y, Bae C, An K, Park J G, Park H M and Hyeon T 2004 *Angew. Chem.* **116** 2332

[138] Vanitha P V and O'Brien P 2008 *J. Am. Chem. Soc.* **130** 17256

[139] Zhang Y, Du Y, Xu H and Wang Q 2010 *CrystEngComm* **12** 3658

[140] Ghezelbash A, Sigman M B and Korgel B A 2004 *Nano Lett.* **4** 537

[141] Oyler K D, Ke X, Sines I T, Schiffer P and Schaak R E 2009 *Chem. Mater.* **21** 3655

[142] Bi Y, Yuan Y, Exstrom C L, Darveau S A and Huang J 2011 *Nano Lett.* **11** 4953

[143] Chen L, Zhan H, Yang X, Sun Z, Zhang J, Xu D, Liang C, Wu M and Fang J 2010 *Cryst. Eng. Comm.* **12** 4386

[144] Zhang H, Long G, Li D, Sabirianov R and Zeng H 2011 *Chem. Mater.* **23** 3769

[145] Polshettiwar V, Luque R, Fihri A, Zhu H B, Bouhrara M and Bassett J M 2011 *Chem. Rev.* **111** 3036

[146] Zeng H, Sun S H, Li J, Wang Z L and Liu J P 2004 *Appl. Phys. Lett.* **85** 792

[147] Chaubey G S, Nandwana V, Poudyal N, Rong C B and Liu J P 2008 *Chem. Mater.* **20** 475

[148] Schladt T D, Graf T, Kohler O, Bauer H, Dietzsch M, Mertins J, Branscheid R, Kolb U and Tremel W 2012 *Chem. Mater.* **24** 525

[149] Salazar-Alvarez G, Lidbaum H, Lopez-Ortega A, Estrader M, Leifer K, Sort J, Surinach S, Baro M D and Nogues J 2011 *J. Am. Chem. Soc.* **133** 16738

[150] Song Q and Zhang Z J 2012 *J. Am. Chem. Soc.* **134** 10182

[151] Zeng H, Li J, Wang Z L, Liu J P and Sun S H 2004 *Nano Lett.* **4** 187

[152] Shi W, Zeng H, Sahoo Y, Ohulchanskyy T Y, Ding Y, Wang Z L, Swihart M and Prasad P N 2006 *Nano Lett.* **6** 875

[153] Hou Y L, Xu Z C, Peng S, Rong C B, Liu J P and Sun S H 2007 *Adv. Mater.* **19** 3349

[154] Teng X W, Black D, Watkins N J, Gao Y L and Yang H 2003 *Nano Lett.* **3** 261

[155] Zhou T, Lu M, Zhang Z, Gong H, Chin W S and Liu B 2010 *Adv. Mater.* **22** 403

[156] Sun X L, Huls N F, Sigdel A and Sun S H 2012 *Nano Lett.* **12** 246

[157] Masala O and Seshadri R 2005 *J. Am. Chem. Soc.* **127** 9354

[158] Xu Z C, Hou Y L and Sun S H 2007 *J. Am. Chem. Soc.* **129** 8698

[159] Gu H, Zheng R, Zhang X and Xu B 2004 *J. Am. Chem. Soc.* **126** 5664

[160] Gao J H, Zhang B, Gao Y, Pan Y, Zhang X X and Xu B 2007 *J. Am. Chem. Soc.* **129** 11928

[161] Lee J S, Bodnarchuk M I, Shevchenko E V and Talapin D V 2010 *J. Am. Chem. Soc.* **132** 6382

[162] Guerrero-Martinez A, Perez-Juste J and Liz-Marzan L M 2010 *Adv. Mater.* **22** 1182

[163] Selvan S T, Patra P K, Ang C Y and Ying J Y 2007 *Angew. Chem. Int. Ed.* **46** 2448

[164] Lee D C, Mikulec F V, Pelaez J M, Koo B and Korgel B A 2006 *J. Phys. Chem. B* **110** 11160

[165] Vestal C R and Zhang Z J 2003 *Nano Lett.* **3** 1739

[166] Yi D K, Lee S S, Papaefthymiou G C and Ying J Y 2006 *Chem. Mater.* **18** 614

[167] Cannas C, Musinu A, Ardu A, Orru F, Peddis D, Casu M, Sanna R, Angius F, Diaz G and Piccaluga G 2010 *Chem. Mater.* **22** 3353

[168] Tracy J B, Weiss D N, Dinega D P and Bawendi M G 2005 *Phys. Rev. B* **72** 064404

[169] Johnston-Peck A C, Wang J W and Tracy J B 2009 *Acs Nano* **3** 1077

[170] Lee W R, Kim M G, Choi J R, Park J I, Ko S J, Oh S J and Cheon J 2005 *J. Am. Chem. Soc.* **127** 16090

[171] Salazar-Alvarez G, Sort J, Surinach S, Baro M D and Nogues J 2007 *J. Am. Chem. Soc.* **129** 9102

[172] Sobal N S, Hilgendorff M, Möhwald H, Giersig M, Spasova M, Radetic T and Farle M 2002 *Nano Lett.* **2** 621

[173] Carroll K J, Calvin S, Ekiert T F, Unruh K M and Carpenter E E 2010 *Chem. Mater.* **22** 2175

[174] Wang D S and Li Y D 2010 *J. Am. Chem. Soc.* **132** 6280

[175] Lai J, Shafi K V P M, Ulman A, Loos K, Popovitz-Biro R, Lee Y, Vogt T and Estournès C 2005 *J. Am. Chem. Soc.* **127** 5730

[176] Yu H, Chen M, Rice P M, Wang S X, White R L and Sun S H 2005 *Nano Lett.* **5** 379

[177] Shi W L, Zeng H, Sahoo Y, Ohulchanskyy T Y, Ding Y, Wang Z L, Swihart M and Prasad P N 2006 *Nano Lett.* **6** 875

[178] Jiang J, Gu H W, Shao H L, Devlin E, Papaefthymiou G C and Ying J Y 2008 *Adv. Mater.* **20** 4403

[179] Choi S H, Bin Na H, Park Y I, An K, Kwon S G, Jang Y, Park M, Moon J, Son J S, Song I C, Moon W K and Hyeon T 2008 *J. Am. Chem. Soc.* **130** 15573

[180] Wang C, Yin H F, Dai S and Sun S H 2010 *Chem. Mater.* **22** 3277

[181] Wei Y H, Klajn R, Pinchuk A O and Grzybowski B A 2008 *Small* **4** 1635

[182] Zhang L, Dou Y H and Gu H C 2006 *J. Colloid Interface Sci.* **297** 660

[183] Schladt T D, Shukoor M I, Schneider K, Tahir M N, Natalio F, Ament I, Becker J, Jochum F D, Weber S, Kohler O, Theato P, Schreiber L M, Sonnichsen C, Schroder H C, Muller W E G and Tremel W 2010 *Angew. Chem. Int. Ed.* **49** 3976

[184] He S L, Zhang H W, Delikanli S, Qin Y L, Swihart M T and Zeng H 2009 *J. Phys. Chem. C* **113** 87

[185] Choi J S, Jun Y W, Yeon S I, Kim H C, Shin J S and Cheon J 2006 *J. Am. Chem. Soc.* **128** 15982

[186] Zanella M, Falqui A, Kudera S, Manna L, Casula M F and Parak W J 2008 *J. Mater. Chem.* **18** 4311

[187] Gu H W, Zheng R K, Zhang X X and Xu B 2004 *J. Am. Chem. Soc.* **126** 5664

[188] Kwon K W, Lee B H and Shim M 2006 *Chem. Mater.* **18** 6357

[189] Kwon K W and Shim M 2005 *J. Am. Chem. Soc.* **127** 10269

[190] McDaniel H and Shim M 2009 *ACS Nano* **3** 434

[191] Gu H W, Yang Z M, Gao J H, Chang C K and Xu B 2005 *J. Am. Chem. Soc.* **127** 34

[192] Teranishi T, Inoue Y, Nakaya M, Oumi Y and Sano T 2004 *J. Am. Chem. Soc.* **126** 9914

[193] Figuerola A, Fiore A, Di Corato R, Falqui A, Giannini C, Micotti E, Lascialfari A, Corti M, Cingolani R, Pellegrino T, Cozzoli P D and Manna L 2008 *J. Am. Chem. Soc.* **130** 1477

[194] Wu J, Hou Y and Gao S 2011 *Nano Res.* **4** 836

[195] Buonsanti R, Grillo V, Carlino E, Giannini C, Curri M L, Innocenti C, Sangregorio C, Achterhold K, Parak F G, Agostiano A and Cozzoli P D 2006 *J. Am. Chem. Soc.* **128** 16953

[196] Buonsanti R, Grillo V, Carlino E, Giannini C, Gozzo F, Garcia-Hernandez M, Garcia M A, Cingolani R and Cozzoli P D 2010 *J. Am. Chem. Soc.* **132** 2437

[197] Buonsanti R, Snoeck E, Giannini C, Gozzo F, Garcia-Hernandez M, Garcia M A, Cingolani R and Cozzoli P D 2009 *PCCP* **11** 3680

[198] Maynadie J, Salant A, Falqui A, Respaud M, Shaviv E, Banin U, Soulantica K and Chaudret B 2009 *Angew. Chem. Int. Ed.* **48** 1814

[199] Jen-La Plante I, Habas S E, Yuhas B D, Gargas D J and Mokari T 2009 *Chem. Mater.* **21** 3662

[200] Habas S E, Yang P D and Mokari T 2008 *J. Am. Chem. Soc.* **130** 3294

[201] Yuhas B D, Habas S E, Fakra S C and Mokari T 2009 *ACS Nano* **3** 3369

[202] Kostopoulou A, Thétiot F, Tsiaoussis I, Androulidaki M, Cozzoli P D and Lappas A 2012 *Chem. Mater.* **24** 2722

[203] Deka S, Falqui A, Bertoni G, Sangregorio C, Poneti G, Morello G, De Giorgi M, Giannini C, Cingolani R, Manna L and Cozzoli P D 2009 *J. Am. Chem. Soc.* **131** 12817

[204] Casavola M, Falqui A, Garcia M A, Garcia-Hernandez M, Giannini C, Cingolani R and Cozzoli P D 2009 *Nano Lett.* **9** 366

[205] Casavola M, Grillo V, Carlino E, Giannini C, Gozzo F, Pinel E F, Garcia M A, Manna L, Cingolani R and Cozzoli P D 2007 *Nano Lett.* **7** 1386

[206] Yin Y, Rioux R M, Erdonmez C K, Hughes S, Somorjai G A and Alivisatos A P 2004 *Science* **304** 711

[207] Bang J H and Suslick K S 2007 *J. Am. Chem. Soc.* **129** 2242

[208] Yu T, Park J, Moon J, An K, Piao Y and Hyeon T 2007 *J. Am. Chem. Soc.* **129** 14558

[209] Peng S and Sun S 2007 *Angew. Chem.* **119** 4233

[210] Cheng K, Peng S, Xu C and Sun S 2009 *J. Am. Chem. Soc.* **131** 10637

[211] Cabot A, Puntes V F, Shevchenko E, Yin Y, Balcells L, Marcus M A, Hughes S M and Alivisatos A P 2007 *J. Am. Chem. Soc.* **129** 10358

[212] An K, Kwon S G, Park M, Na H B, Baik S I, Yu J H, Kim D, Son J S, Kim Y W, Song I C, Moon W K, Park H M and Hyeon T 2008 *Nano Lett.* **8** 4252

[213] Kim D, Park J, An K, Yang N K, Park J G and Hyeon T 2007 *J. Am. Chem. Soc.* **129** 5812

[214] Zhao J, Jian Z, Ma J, Wang F, Hu Y S, Chen W, Chen L, Liu H and Dai S 2012 *ChemSusChem* **5** 1495

[215] Shin J, Anisur R M, Ko M K, Im G H, Lee J H and Lee I S 2009 *Angew. Chem. Int. Ed.* **48** 321

[216] Kim T, Momin E, Choi J, Yuan K, Zaidi H, Kim J, Park M, Lee N, McMahon M T, Quinones-Hinojosa A, Bulte J W M, Hyeon T and Gilad A A 2011 *J. Am. Chem. Soc.* **133** 2955

[217] Peng Y K, Lai C W, Liu C L, Chen H C, Hsiao Y H, Liu W L, Tang K C, Chi Y, Hsiao J K, Lim K E, Liao H E, Shyue J J and Chou P T 2011 *ACS Nano* **5** 4177

[218] Hao R, Yu J, Hou Y and Sun S 2011 *Chem. Commun.* **47** 9095

[219] Yu J, Hao R, Sheng F, Xu L, Li G and Hou Y 2012 *Nano Res.* **5** 679